

# **Antimicrobial Polymer-Nanocomposite Coating to Combat Catheter-Associated Urinary Tract Infections (CAUTIs)**

A thesis

Submitted in partial fulfilment for the Degree of

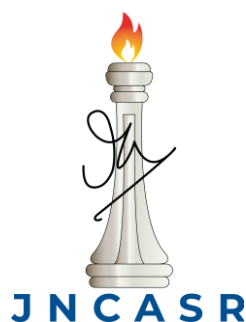
**Master of Science**

as a part of Integrated Ph.D. programme

in Materials Science

by

**Dipanjana Patra**



Chemistry and Physics of Materials Unit

Jawaharlal Nehru Centre for Advanced Scientific Research

Bangalore - 560 064

March 2022

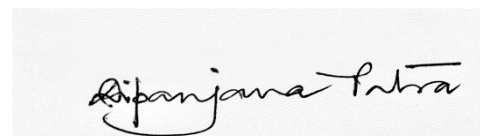


*To my parents*



## DECLARATION

I hereby declare that the matter embodied in the thesis entitled “**Antimicrobial Polymer-Nanocomposite Coating to Combat Catheter-Associated Urinary Tract Infections (CAUTIs)**” is the result of investigations carried out by me at the New Chemistry Unit, Jawaharlal Nehru Centre for Advanced Scientific Research, Bangalore, India under the supervision of Prof. Jayanta Haldar and that it has not been submitted elsewhere for the award of any degree or diploma. In keeping with the general practice in reporting scientific observations, due acknowledgement has been made whenever the work described is based on the findings of other investigators.



---

Dipanjana Patra



## CERTIFICATE

I hereby certify that the matter embodied in this thesis entitled “**Antimicrobial Polymer-Nanocomposite Coating to Combat Catheter-Associated Urinary Tract Infections (CAUTIs)**” has been carried out by Ms. Dipanjana Patra at the New Chemistry Unit, Jawaharlal Nehru Centre for Advanced Scientific Research, Bangalore, India under my supervision and that it has not been submitted elsewhere for the award of any degree or diploma.



---

Prof. Jayanta Halder  
(Research Supervisor)





## Acknowledgements

Firstly, I want to thank my research supervisor, Prof. Jayanta Haldar for his constant support, guidance, and freedom that he had offered me to explore new things. His insights and knowledge never cease to amaze me. I am extremely grateful to him for making me a part of his lab and giving me enough confidence to take up new challenges every day.

I have been extremely fortunate to be in the same campus with Bharat Ratna, Prof. C.N.R. Rao. An enigma whose kind words have motivated many young minds like me.

I would like to thank my parents for their wise counsel and sympathetic ear. You are always there for me when I must complain about the smallest of things or share the smallest of achievements. I wouldn't have come this far if it wasn't for the two of you.

I want to thank my course instructors, Prof. Subi George (NCU), Prof. Jayanta Haldar (NCU), Prof. Shobhana Narasimhan (TSU), Prof. Rajesh Ganapathy (CPMU), Prof. Sarit Agasti (NCU), Prof. Sundaresan (CPMU), Prof. Chandrabhas Narayana (CPMU), Prof. N.S. Vidhyadhiraja (TSU), Prof. Kavita Jain (TSU), Prof. Premkumar Senguttuvan (NCU), Prof. Sridhar Rajaram (NCU), Prof. Eshwaramoorthy (CPMU), Prof. Bivas Saha (CPMU), Prof. Swapan K. Pati (TSU), Prof. Ranjan Datta (CPMU), Prof. U. Waghmare (TSU), for teaching me to be analytical and approach problems scientifically. I am extremely grateful to them for helping me expand the horizon of knowledge.

I want to thank all my lab mates, for making me feel like home away from home. I extend my gratitude to alumni members, Jiaul, CD, Venky, Diwakara, Paramita, Swagatam, Brinta, Riya. I want to thank my present lab family, Sreyan, Rajib, Geetika, Sudip, Yash, Subhankar, Nandini, Sayan, Saurav, Vinayak, Sucheta, Logia. Especially, Sreyan Ghosh (co-boss), who has tolerated my

innumerable tantrums and has entertained my shenanigans on a daily basis. Without, his unconditional love, support, and guidance, I probably wouldn't have had a thesis.

I would like to thank Manodeep Mondal and Niloyendu Roy, for being one of the best seniors in JNC. I would also like to thank, Soumi Mondal for being a very supportive roommate and lending a sympathetic ear.

I would finally love to thank my batchmates, Aashish, Uttam, Surabhi, Animesh, Tarak, Aditya, Anustup, Amit, Vinay, Sohini and Arif for making me laugh when I was down.

I would like to extend my gratitude to academic, administration, technical, security, library, complab and Dhanvantri people for making life in JNC easy.

# Chapter 1

## Introduction



## 1.1. Urinary Tract Infection (UTI)

Infectious diseases are a serious threat to human health and a huge burden on the global economy. A troublesome class of infections that are caused by contaminated fomites or invasive medical devices from the hospitals, known as nosocomial infections or hospital-acquired infections (HAIs), present a severe challenge in the healthcare setting. The various infections that contribute to HAIs are surgical site infections (SSIs), bloodstream infections, urinary tract infections (UTIs), pneumoniae, adverse effects to drugs, etc. and lead to a heavy financial burden on the patient's family (Figure 1.1).

Urinary tract infections (UTIs) are among the most prevalent hospital-acquired bacterial diseases, affecting more than 150 million individuals globally each year.<sup>1</sup> In 2007, there were an estimated 10.5 million hospital visits for UTI symptoms and 2–3 million emergency room visits in the United States alone. In the United States alone, the societal costs of these infections, including health-care expenditures and lost time at work, are currently estimated to be over US\$3.5 billion per year. UTIs are also a major source of morbidity in children, elderly men, and women of all ages. Recurrences, pyelonephritis with sepsis, kidney injury in young infants, pre-term delivery, and problems related by repeated antimicrobial

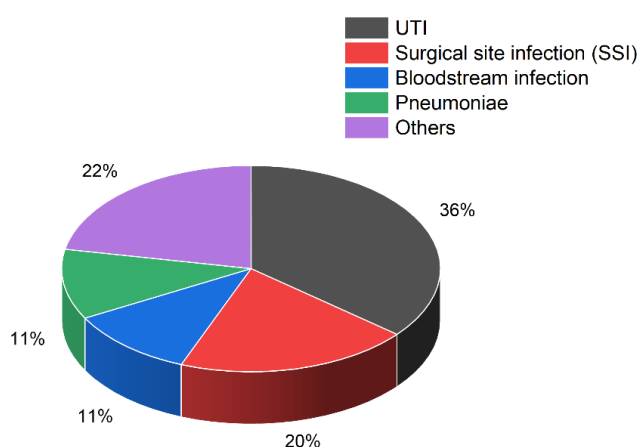


**Figure 1.1:** Most common nosocomial infections.

usage, such as high-level antibiotic resistance and *Clostridium difficile* colitis, are all serious consequences.<sup>2</sup>

UTI is categorized majorly as uncomplicated and complicated on the basis of increasing colonization and decreasing efficacy of therapy. Lower UTIs (cystitis) and higher UTIs (pyelonephritis) are the two types of uncomplicated UTIs that affect people who are generally healthy and have no anatomical or neurological urinary tract abnormalities. Women suffer from UTI more often than men, also if one has suffered from previous UTI, sexual activity, vaginal infection, diabetes, obesity, and genetic predisposition are all risk factors for cystitis.<sup>3</sup> Urine blockage, urinary retention caused by neurological illness, immunosuppression, renal failure, renal transplantation, pregnancy, and the presence of foreign bodies such as calculi, indwelling catheters, or other drainage devices are all examples of complicated UTIs.<sup>3</sup> CAUTIs (catheter-associated urinary tract infections) are the most prevalent cause of subsequent bloodstream infections, with increased morbidity and death. Prolonged catheterization, feminine gender, older age, and diabetes are all risk factors for CAUTI.

## **1.2. Mechanism of infection**

Various mice models have been developed in the last 20 years to better understand the molecular underpinnings of UTI aetiology.<sup>3</sup> Knowledge acquired from these studies have been easily translated to human subjects.<sup>4</sup> After reaching the lumen of the urinary bladder, the uropathogenic bacteria responsible for UTI, adhere to the surface of the superficial ‘umbrella cells’, also known as facet cells which line the bladder, using adhesive filamentous extensions (FimH) called ‘type 1 pili’. On attachment to the bladder lining, the bacteria are integrated into the epithelial cells, where they multiply in number to form biofilm-like intracellular bacterial communities (IBCs). Here, the bacteria can dodge Toll-like receptor 4 (TLR4)- mediated expulsion and replicate in the cytoplasm of the urothelial cell before they can undergo

filamentation and re-enter the bladder lumen and stick to the nearby cells, leading to clonal expansion which can initiate a new infection cycle (Figure 1.2).<sup>5,6</sup>

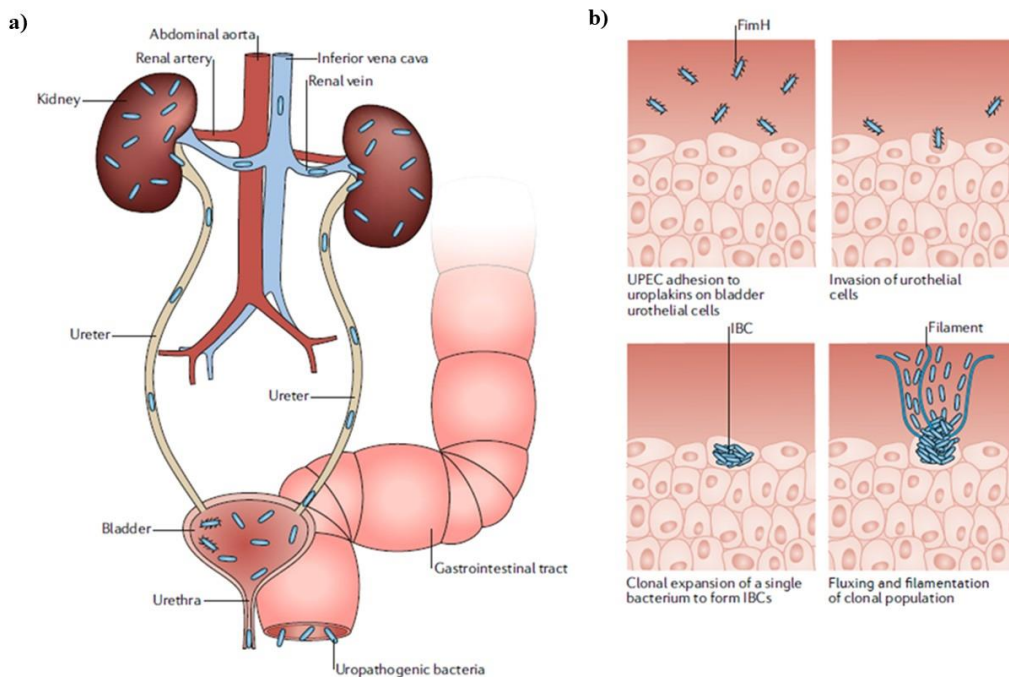


**Figure 1.2:** Pathogenesis of UTI by uropathogenic bacteria in a nutshell. a) Uropathogenic bacteria invades and colonizes the bladder by ascending the urethra. b) Individual bacteria stick to and infiltrate superficial urothelial umbrella cells of the bladder through FimH receptors. They clonally expand to create biofilm-like intracellular bacterial communities (IBCs) which help start a new infection cycle. Figure reproduced with permission from reference 3. Copyright 2020 Nature Publishing Group.

In response to the host secretion of various pro-inflammatory cytokines like interleukin-6 (IL-6), IL-17, tumour necrosis factor (TNF), the migration of neutrophil recruitment into the uroepithelium is initiated. This eventually leads to monocyte invasion and a programmed apoptosis and exfoliation which might decrease the bacterial burden but leads to mucosal damage, accompanied with chronic inflammation.<sup>7-10</sup>

### **1.3. Catheter-associated urinary tract infections (CAUTIs)**

Invasive medical devices, such as urinary catheters, are linked to more than 75% of nosocomial infections, resulting in catheter-associated urinary tract infections (CAUTIs). CAUTIs cause a 2.3% mortality rate. Cross-contamination from drainage bags and external pathogenic contamination coming from skin and other ambient surfaces during catheter handling make a patient extremely vulnerable to catheter-related illnesses. The most common microorganisms responsible for biofilm formation on urinary catheters are various Gram-negative and Gram-positive bacteria like *Escherichia coli*, *Klebsiella pneumoniae*, *Enterococcus faecalis*, *Staphylococcus epidermidis*, and *Proteus mirabilis*.<sup>11</sup>

Bacteria cling to the catheter surface and proliferate, resulting in encrustation. Treatment has grown more complicated due to the advent of multiantibiotic-resistant enterococcal strains and their capacity to build biofilms on catheters (Figure 1.3). Catheterization for a long period of time can cause biofilm development, in which the associated bacteria make extracellular polymeric matrix, colonizing the surface, and allowing the bacterial community to grow and feed on the nutrients provided by the moderate flow of warm urine via the catheter.<sup>12</sup> There have only been a few reports of antimicrobial polymeric catheter coatings that are efficient at penetrating and disrupting biofilms developed on the catheter.<sup>13,14</sup> These bacteria embedded in the biofilm are resistant to conventional drugs due to the biofilm matrix, and less vulnerable to human immune system cells and molecules than their planktonic counterparts. As a result, substantially larger antibiotic doses are necessary to eradicate the bacteria and clear the infection. Typically, catheters are replaced on a regular basis to avoid infection, or the patient is prescribed a dosage regimen of broad-spectrum antibiotics; both options are undesirable since they are tedious or may promote the development of antibiotic resistance and bring further agony to the patient.<sup>15</sup> If CAUTIs are not treated, the condition becomes more serious, with the risk of infection in kidneys and potential sepsis.<sup>3</sup>



The elevation of the urinary pH due to the presence of the uropathogenic bacteria hydrolyses the urea in the urine when the biofilm is formed. The formation of crystals and precipitation of calcium and magnesium phosphates encrusts the surfaces and blocks the catheters.<sup>16</sup> Catheterization alters the bladder ecology accompanied by various histological and immunological changes, sometimes leading to the foreign body response and eventually

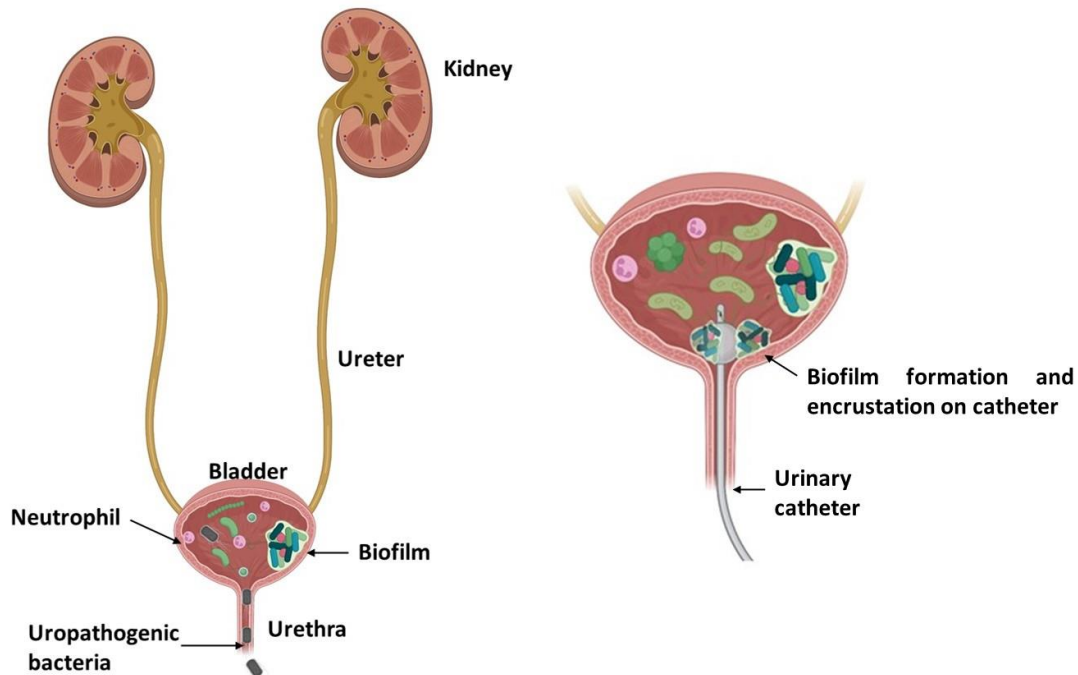


**Figure 1.3:** Urinary tract of humans. Urinary tract infections (UTIs) begin with the contamination of the periurethral area with uropathogenic bacteria migration from the gut. Catheter-associated UTIs are one of the most common UTIs. Due to ecological change in the bladder, it leads to protein and salt deposition, biofilm encrustation and potential epithelium damage.

generation of fibrinogen.<sup>13</sup> As a part of the host's inflammatory response, fibrinogen is released into the bladder during catheterization, where it accumulates and gets deposited on the implanted catheter. The inflammatory response is mediated by IL-6, IL-1 $\beta$ , IL-8, and TNF- $\alpha$ .

Fibrinogen deposition is exploited by urinary pathogens in a variety of ways. *Enterococci* attach directly to fibrinogen with special appendages, Ebp pili, then employ the GelE and SprE proteases to increase fibrinogen cleavage using fibrinogen as a food supply. Clumping factor B (ClfB) is used by *Staphylococci* to attach to the fibrinogen-coated catheter and cause bladder inflammation. Finally, FimH adhesin is used by *Escherichia coli* to bind fibrinogen covering the catheters.<sup>17-19</sup>

Intensive efforts have been made to reduce any bacterial buildup on the catheter surface. These strategies can be classified as active or passive techniques. Antimicrobial coatings capable of interfering with biological pathways are used in most active activities.<sup>17</sup> One of the most facile methods for loading active compounds onto catheters involves the impregnation of the catheter surface with antimicrobial agents which exert their antibacterial activity by leaching out from the surfaces.<sup>20</sup> Antimicrobial and antifouling materials are the focus of catheter research because they have shown promise in providing overall protection against CAUTIs because to their high cytotoxicity.<sup>20</sup> Although this is a complex problem, materials that combine known antimicrobial agents show an increased effectiveness against CAUTIs. The materials described herein are not an exhaustive list, instead, a highlight of the major materials used to combat CAUTIs.

#### **1.4. Release-based coatings**

One of the most facile methods for loading active compounds involves the impregnation of the catheter surface with antimicrobial agents which exert their antibacterial activity by leaching out the loaded compounds that kills both adhered and planktonic bacteria. The release is attained by diffusion of the antibacterial agents into aqueous medium, degradation or even

hydrolysis of covalent bonds (Figure 1.4). Elution directly from the surface offers a better chance to deliver a higher concentration of the compound locally, maintaining toxicity levels.

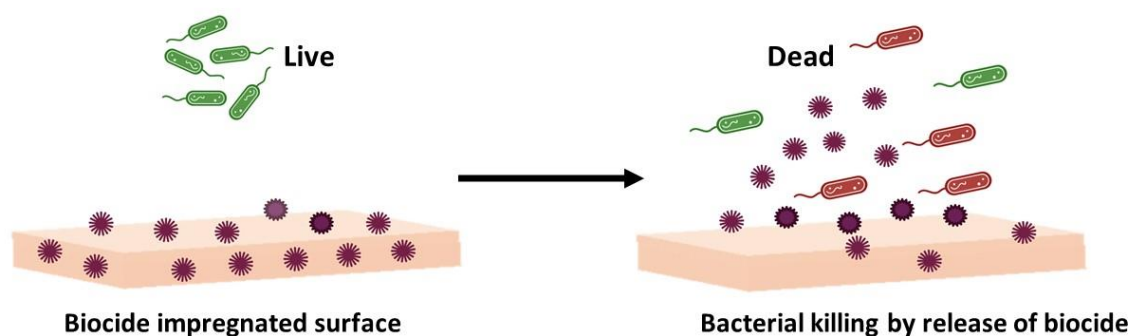


**Figure 1.4:** Schematic representation of release-based coating. Different antimicrobial biocides are impregnated onto the surface, and upon release, lead to death of bacteria.

Ideally, there should be fast drug release at the initial stage to kill the bacteria in the vicinity, preventing any kind of biofilm formation, hence maintaining a slow and prolonged drug activity. This aids in preventing any encrustation or biofilm formation. Release-based coatings have proven to be a focal point of research in combating CAUTIs.<sup>21</sup>

### 1.4.1. Antibiotics

Antibiotics or antibacterial agents are medications that can destroy or retard the growth of bacteria. Antibiotics are entrapped into invasive medical devices, via two major processes, firstly, a layer of antibiotics is coated on surface followed by the rapid elution of the drug and secondly, by the direct impregnation of the antibiotics into the device polymer during its manufacturing with or without the inclusion of excipients that can slow down or accelerate the rate of drug release.<sup>22-24</sup> Anionic derivatives are designed in such a way that the anionic charges allow for easy electrostatic binding to the surface, resulting in increased solubility..<sup>25,26</sup> Polyurethane catheters modified with antibiotics were developed by adsorbing cefamandole and vancomycin onto the surface, which in turn enhanced catheter resistance against microbial

infections.<sup>26,27</sup> An approved drug that has showed efficacy against UTI is nitrofurazone. When Foley catheters were impregnated with nitrofurazone, it was marketed for commercial use. It showed effective killing of *E. coli* bacteria in the first week compared to an uncoated catheter, and even better activity than a silver alloy coated catheter.<sup>20,28</sup>

Sparfloxacin, an antibiotic of the class of fluoroquinolones, was immobilized onto heparin-coated silicone latex catheter by oxidizing with sodium periodate and by linkage of antibiotic in an organic medium. The catheters were non-toxic and inhibited biofilm formation.<sup>29</sup> Antibiotic-impregnated catheters have emerged as a great alternative; however, frequent usage can lead to antibiotic resistance. As a result, only certain quantities and kinds of antibiotics may be employed, limiting the antibacterial range. To proceed with antibiotic-loaded catheters, a more comprehensive and fluent knowledge is necessary.

#### **1.4.2. Antiseptics**

Chlorhexidine (CHX), a cationic bisguanide, has been commonly used as an agent to prevent biofilms and as a catheter coating to prevent catheter-associated urinary tract infections (CAUTIs).<sup>20,30</sup> Another broad-spectrum antimicrobial agent, commonly used in consumer products, is Triclosan. At lower concentrations, it is bacteriostatic and at higher concentrations it has biocidal properties. Triclosan, when used in a fluidic form filled into the retention balloon of the catheter, and by impregnating it into the coating of the catheter material.<sup>31</sup> Evaporation and dip-method were used as the coating process as triclosan is organo-soluble.<sup>32</sup> When compared to a nitrofurazone catheter, a silicone catheter loaded with CHX, silver sulfadiazine, and triclosan is far more successful in stopping the colony growth of *S. aureus* and *S. epidermidis* for a longer period (23–24 days).<sup>33</sup> Trials to eradicate encrustation caused by *P. mirabilis*, triclosan loaded polyurethane samples were prepared, which exhibited higher antimicrobial

activity by lowering the pH of the urine.<sup>34</sup> Due to certain hormonal dysregulation in certain animal studies, this approach is still up for discussion.<sup>20</sup>

### **1.4.3. Silver**

Silver is one of the most often utilised antibacterial treatments for urinary catheters. It is a powerful biocide and a desirable agent for invasive medical devices because of its numerous mechanistic methods. Ag alloys with noble metals such as gold and palladium, Ag-containing polymers, nanoparticles, and even some nanocomposites are used to create silver-ion release-based coatings.<sup>21,29,35,36</sup>

For urogenital uses, silver-based alloy coatings on catheters are being used, with antibiotics like nitrofurantoin. When compared to nitrofurantoin-coated catheters, the adhesion of numerous CAUTI-causing microorganisms on silver-alloy coated catheters was efficient against bacterial adherence as well as biofilm formation.<sup>37</sup> Comparatively, Ag-PTFE coated catheters showed enhanced antimicrobial properties along with anti-adhesion properties due to its synergistic effects of silver and polytetrafluoroethylene. As compared to market available silicone catheters, silver and Ag-PTFE coated catheters, bacterial adhesion significantly decreased.<sup>38</sup>

Even though silver nanoparticles have gained massive popularity in the scientific research community to combat infections and bacterial resistance, it has its set of drawbacks like its high costs and absence of reliable reports. Alongside, silver shows cytotoxicity, therefore new combinations are being designed that can substantially increase the antimicrobial efficacy and significantly decrease cytotoxicity.<sup>20</sup>

### **1.4.4. Nitric oxide**

Nitric oxide, which is created in endothelial cells by the enzymatic oxidation of L-arginine by NO synthase, has proved to be an efficient antibacterial agent, with increased production during

infections. S-nitrosothiols such as S-nitroso-*N*-acetyl-D, L penicillamine (SNAP), and S-nitrosoglutathione (GSNO) are often utilised as nitric oxide donors. Because of the molecule's high reactivity, prolonged release in its native state is challenging, thus the donor molecules are either covalently bonded to the surface or non-covalently integrated with polymers.<sup>39-41</sup>

SNAP has shown promising results because NO releases up to 3 weeks as solvent form of SNAP impregnation into the polymer showed a controlled release for a period of 14 days and reduced bacterial growth of *S. epidermidis* and *P. aeruginosa*.<sup>42</sup> Many Foley catheters have been impregnated with SNAP showed a sustained release for 30 days and showed effective antimicrobial activity as compared to silver-alloy based coatings and an equivalent activity compared to nitrofurazone coated catheters.<sup>28</sup> Nevertheless, NO-releasing coatings have an adverse effect on the human body like inhibition of platelet aggregation, skin oedema and even blood pressure reduction.<sup>40</sup>

## **1.5. Contact-based coatings**

Among the different strategies for biofilm prevention, the use of non-eluting surfaces that counteract bacterial attachment and kill bacterial cells have shown longer antimicrobial durability and lesser toxicity. Antimicrobial agents, mainly, cationic enzymes or molecules, are covalently attached to the catheter surface through hydrophobic polymeric chains. They show contact-killing mechanism by disrupting the bacterial membrane through membrane interactions (Figure 1.5). Prolonged activity is observed without any interference with the host immune responses since cationic functional groups are stable.<sup>43</sup>

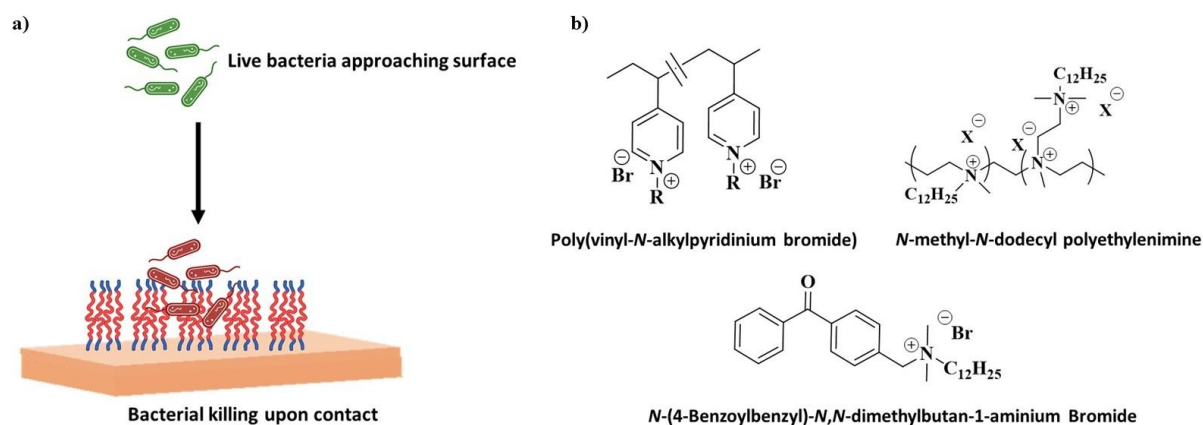


**Figure 1.5:** a) Schematic representation of contact-active coating, wherein the active antimicrobial immobilized on the surface kills pathogens upon contact b) Structures of various quaternary polymers used in the development of contact-active surfaces.

### 1.5.1. Chitosan

Chitosan a naturally available linear cationic polysaccharide with non-toxic, antibacterial, and antifouling properties. It has been greatly exploited as a drug carrier and even as a contact-based coating against bacteria. Its low molecular weight form facilitates it to penetrate the bacterial cell walls and eventually bind with DNA and high molecular weight chitosan acts through electrostatic interactions between the positively charged and the negatively charged components on the microbial membranes altering the cell permeability and transport into the cell.<sup>44,45</sup>

Chitosan has the capability to reduce bacterial adhesion and regrowth of any Gram-negative uropathogenic bacteria. A considerable reduction in *E. coli* and *K. pneumoniae* viability and increasing the activity with lower pH and molecular weight of the chitosan solution medium. It is also able to electrostatically bind to anionic antibiotic molecules such as

rifampicin, to form a slow and controlled release system linked with drugs with high efficiency. A chitosan can be used effectively for preventing any fungal biofilm.<sup>45,46</sup>

### **1.5.2. Quaternary ammonium compounds**

One of the most promising antimicrobial approaches is quaternary ammonium compounds (QAC). QACs are cationic in nature, bearing a nitrogen that is covalently linked to four alkyl groups. In these molecules, a direct correlation between efficacy of these cationic polymers and length of the chains is observed. Their mechanism of action isn't clearly understood still but it has been deciphered that it is related to the disruption of cell membrane disruption, cellular lysis and even the moderation of cell surface charges.<sup>47</sup> In viruses, QACs act by disrupting the viral envelope and leading to release of the nucleocapsid. Despite the limited reports describing QAC-based strategies applied against CAUTIs, there have been studies describing polyurethane and silicone surfaces. There have been many grafting processes that made the materials permanently biocidal. This process involves the direct immobilization of molecules on the surface or polymerization reactions that increase the polymer's density.<sup>48-50</sup>

Pant et al. has functionalized a multi-defence strategy of incorporating SNAP as the NO donor in a CarboSil polymeric composite with a benzophenone-based quaternary ammonium coating. There have been many novel approaches too, that involves a plasma-based method to develop quaternary ammonium silane (QAS) on catheters too.<sup>51</sup>

### **1.5.3. Antimicrobial peptides**

Antimicrobial peptides (AMPs) are short-stranded peptides with 15-50 amino acids that can be found in prokaryotic and eukaryotic organisms, and shows antimicrobial activity against bacteria, fungi, and even enveloped viruses.<sup>52</sup> AMPs are a part of the innate immune response system and can function as immunomodulators. On analysis, it is known that AMPs are mostly cationic due to the presence of lysine and arginine. They can exhibit their antibacterial



properties by either membrane disruption or by penetrating the membranes and targeting the intracellular constituents. Besides membrane disruption, AMPs can also disturb the DNA, RNA, or protein synthesis when it is translocated through the membrane. In a 2015 study, an AMP, CWR11 was attached to a polydimethylsiloxane (PDMS) film surface taking the help of polydopamine (DOPA).<sup>53-55</sup> The DOPA coating went through oxidative crosslinking, along with chemical bond formation with any surface silanol groups. This was a promising study as the coating prevented any kind of biofilm formation for the next 21 days.<sup>56</sup>

Different architecture of AMP can increase or decrease the antimicrobial activity. To maintain its contact-killing property it must maintain salt resistance, biocompatibility, and antimicrobial activity. It has been observed that AMPs linked with allyl glycidyl ether (AGE) polymer brushes showed no biofilm formation and was more effective and rapid in killing than any ordinary immobilized peptides. A system was designed by immobilizing the AMP Chain201D from crowberries on a model of self-assembled monolayer surfaces.<sup>57</sup> Again, a novel polymer-based strategy consisting of highly active AMPs attached to a PDMA-co-APMA brush on a PU catheter that has antifouling properties along with specific flexible sites for any peptide conjugation.<sup>53</sup> It reduced bacterial adhesion by almost 99.99%. In vivo study showed bacterial adhesion reduced by 4 log units and inhibited planktonic bacterial growth by 3 log units.

AMPs have given rise to many antimicrobial agents because of its resistance mechanisms. However, some of the issues with them are their substandard coating properties, potential toxicity, pH sensitivity and expensive synthesis process.

#### **1.5.4. Enzymes**

The capability of enzymes to destroy biofilms and prevent their initial attachment has made them an active component in antimicrobial coatings. It has been proposed as an alternative to

antibiotics because of their prolonged stability and antimicrobial effect against numerous microorganisms.<sup>58</sup> The impregnation of enzymes on surfaces is either through reversible immobilization or irreversible immobilization. Categorization can be done based on their mechanistic action: a) hydrolytic enzymes that act by degrading the bacterial structural components; b) oxidative enzymes that induce the production of antimicrobial substances and finally, c) quorum quenching enzymes that prevent bacterial quorum sensing.<sup>20</sup>

Lysozyme, a natural component of the innate immune system is a polysaccharide hydrolysing enzyme. It can be found in several secretions like tears or even saliva and acts by catalysing the hydrolysis between N-acetylglucosamine and N-acetylmuramic acid, the main components of the peptidoglycan.<sup>58,59</sup>

Oxidative enzymes produce hydrogen peroxide which is utilized by peroxidases to damage the bacterial cells. The commonly used oxidative enzymes are glucose oxidase, cellobiose dehydrogenase, superoxides, lactoperoxidase.<sup>59</sup> On the other hand, quorum quenching enzymes attack acyl homoserine lactone (AHL), which is the signalling molecule in bacteria. It focuses on disturbing the communication between the bacterial cells, and therefore cannot produce virulence compounds that prevents biofilm formation. In case of catheters or any other invasive medical devices, these enzymes can be immobilized onto the surfaces. Reversible immobilizations include chelation or metal binding by forming the disulphide bonds and adsorption of enzymes through physical bonds. Irreversible methods are preferred due to improved stability and low percentage of leaching.<sup>60</sup>

## **1.6. Dual-active coatings**

The problem of dead bacterial detritus accumulating on quaternary polymeric coatings renders the coatings inert. Release-based coatings work by allowing the loaded components to leak out. Researchers devised a system that demonstrated both the biocide's antibacterial activity as well

as the antimicrobial properties of the polymeric matrix. The polymers can destroy germs that come into touch with them, whereas the biocides that are leached can kill bacteria cells in the immediate vicinity.<sup>38</sup>

Polymer–silver nanocomposites have been shown to be effective against device-related infections, so a highly active dual-functional polymer–silver nanocomposite made of *N, N*-dimethyl-*N*-hexadecyl ammonium chitin tosylate and silver para-toluene sulfonate, which are both antimicrobial and biodegradable, has been developed. Both fungus and bacteria were prohibited from forming biofilms because of the composites discharged into the environment. Methicillin-resistant *Staphylococcus aureus* was successfully combated using nanocomposites (MRSA ATCC 33591). *In vivo* experiments revealed a 2.4 log reduction in MRSA count and a substantial drop in bacterial count based on the amount of polymer–silver nanocomposite coated catheter.<sup>61,62</sup>

Multiple systems have been emerging that are mimics of those found in the nature.<sup>63–65</sup> Certain other properties like self-cleaning, super-wettability rim of a pitcher plant rim,<sup>66</sup> or even the low drag skin of a shark are being explored by scientists.<sup>67</sup>

## **1.7. Scope of thesis**

There is a rising interest in materials that may eliminate dangerous bacteria as a result of the ever-increasing need for healthy living. Surface-associated infections have intensified as a result of increased use of healthcare materials combined with the emergence and spread of antibiotic resistant microorganisms. Various customised antimicrobial surfaces are created and utilised to combat such illnesses. Furthermore, increased use of biomaterials and invasive medical devices (such as catheters, cardiac pacemakers, hip implants, and contact lenses, among others) in combination with contaminated surfaces might result in significant implant-related infections. Different modification principles can be used to modify the surface. Several

surfaces that kill germs by emitting antimicrobials from the surface have been created. These techniques, however, have several drawbacks. The majority of anti-adhesive surfaces are passive by nature. In addition, polymer matrices utilised as antibacterial reservoirs are ineffective against drug-resistant bacterial infections. Fouling, deposition of dead bacterial cells, and proteins on contact-active surfaces deteriorate the surface, rendering it useless over time.

The goal of this thesis is to create antimicrobial materials that overcome the shortcomings of present antibacterial techniques. In Chapter 2, a non-covalent coating, with dual properties have been designed with a polymer and zinc oxide nanoparticles. The one-step surface fabrication has been described with its effective antimicrobial properties and biofilm inhibition properties to combat UTI. The polymer nanocomposite (**APN**) showed effective killing of both Gram-positive and Gram-negative bacteria along with various fungal strains. **APN** has proven to be an effective coating for biomedical devices like urinary catheters. Antimicrobial resistance to such polymer-based coatings is extremely difficult to develop, in contrast to traditional antibiotics. As a result, this coating offers a particularly efficient way to treat urinary tract infections caused by catheters (CAUTIs).





## **Chapter 2**

# **Antimicrobial Polymer-Zinc oxide Nanocomposite Coatings for Rapid Intervention against CAUTIs**





## Abstract

*Chapter 2* describes the synthesis of an organo-soluble antimicrobial polymer nanocomposite (APN) coating for catheters based on quaternized polyethylenimine and zinc oxide nanoparticles which is effective against both UTI causing bacteria and fungi. Simple, spin-coating, dip-coating, and drop-casting methods were incorporated to coat the catheter, silicone, and glass surfaces. The coated surfaces showed ~6 log reduction against both Gram-positive and Gram-negative bacteria like *E. coli*, *K. pneumoniae*, MRSA ATCC 33591, *S. epidermidis*, etc. that are responsible for UTI. The polymer nanocomposite was notably effective also against, fungal strains like *C. albicans* AB226 and *C. albicans* AB399. A surface coated with APN has even shown membrane activity by disrupting the bacterial membrane, along with reactive oxygen species (ROS) generation. In contrast to conventionally used antibiotics, developing any kind of antimicrobial resistance against such polymer-based coatings is very difficult. Hence, this coating presents a very effective method to combat such catheter-associated urinary tract infections (CAUTIs).



## 2.1 Introduction

Urinary tract infections (UTIs) are infections commonly caused by uropathogenic *Escherichia coli* (UPEC) bacteria that enter the urinary tract through the urethral opening, commonly known as the external urethral orifice or urinary meatus before ascending to the urethra finally into the urinary lumen.<sup>3</sup> According to WHO, approximately 50% of women report having UTI at some point in their life leading to an overall annual cost of more than \$1 billion. One of the common UTIs that occur is catheter-associated urinary tract infections (CAUTIs).

Invasive medical devices are responsible for more than 75% of all nosocomial infections. A patient is extremely susceptible to infections produced by a urinary catheter due to cross-contamination from the drainage bag and external pathogenic contamination emerging from the skin and other ambient surfaces during catheterization. The open drainage system in the indwelling catheters bypasses the natural host-defense mechanism and provides the bacteria to colonize the catheters.<sup>2</sup>

Physically embedding coatings on surfaces can sometimes result in leaching and reservoir exhaustion. Our group has developed an antimicrobial paint based on organo-soluble, hydrophobic quaternary polyethyleneimine (PEI) that can fight hospital-acquired diseases. These polymers were coated on glass slides to evaluate their activity against multiple pathogens.<sup>68</sup>

In this study, we have designed a non-covalent-based antimicrobial polymer-nanocomposite (APN) coating with an organo-soluble, hydrophobic quaternized polyethyleneimine (QPEI), from a branched polyethylenimine backbone (750 kDa) functionalized with a hexadecyl amide long chain for common urinary catheter surfaces like silicone incorporated with zinc oxide nanoparticles. The surfaces were characterized with scanning electron microscopy (SEM) and atomic force microscopy (AFM). The coating

showed potent antibacterial and antifungal properties against catheter-associated pathogens like various *E. coli* strains, *Enterococcal* strains, MRSA ATCC 33591, *K. pneumoniae*, *S. epidermidis* and even *Candida* spp. Next, biofilm inhibition studies were conducted against Gram-positive and Gram-negative bacterial strains.

## 2.2. Results and discussion

### 2.2.1. Synthesis and Characterization

**Synthesis of polymer (QPEI) and polymer-nanocomposite (APN).** The polymer, QPEI with a degradable side chain was synthesized by quaternation of *N*-methyl PEI with *N*-hexadecyl-2-bromoethanamide. Firstly, *N*-hexadecyl-2-bromoethanamide was obtained by reacting 1-aminohexadecane with bromoacetyl bromide. Next, *N*-methyl PEI was synthesized via the *Eschweiler-Clarke* methylation scheme of commercially available branched polyethyleneimine (PEI) of N-H peaks ( $3200\text{--}3400\text{ cm}^{-1}$ ) which are present for primary and secondary amine groups. Finally, the *N*-methyl PEI was quaternized with *N*-hexadecyl-2-bromoethanamide to obtain QPEIs with degradable amide sidechain (Figure 2.1 a). They were characterized by FT-IR (Figure 2.1 c) and  $^1\text{H-NMR}$ . Quaternization was confirmed by the complete disappearance of tertiary methyl and methylene protons at around 2.2-2.5 ppm and showed presence of quaternary methyl and methylene protons in the range of 3.2-4.7 ppm.

Zinc oxide nanoparticles were synthesized by reacting zinc acetylacetonate monohydrate with two surfactant moieties oleyl amine and oleic acid under inert conditions (Figure 2.1 b). The obtained nanoparticle was characterized by XRD, which confirmed the formation of nanoparticles with a hexagonal closed packing (hcp) structure, showing significant XRD peaks from  $30^\circ$  to  $80^\circ$  (Figure 2.1 e). The formation of nanoparticles was also confirmed by the observed Zn-O peak around  $480\text{ cm}^{-1}$  in FT-IR. TEM showed an average size of 20 nm for the nanoparticles (Figure 2.1 d).

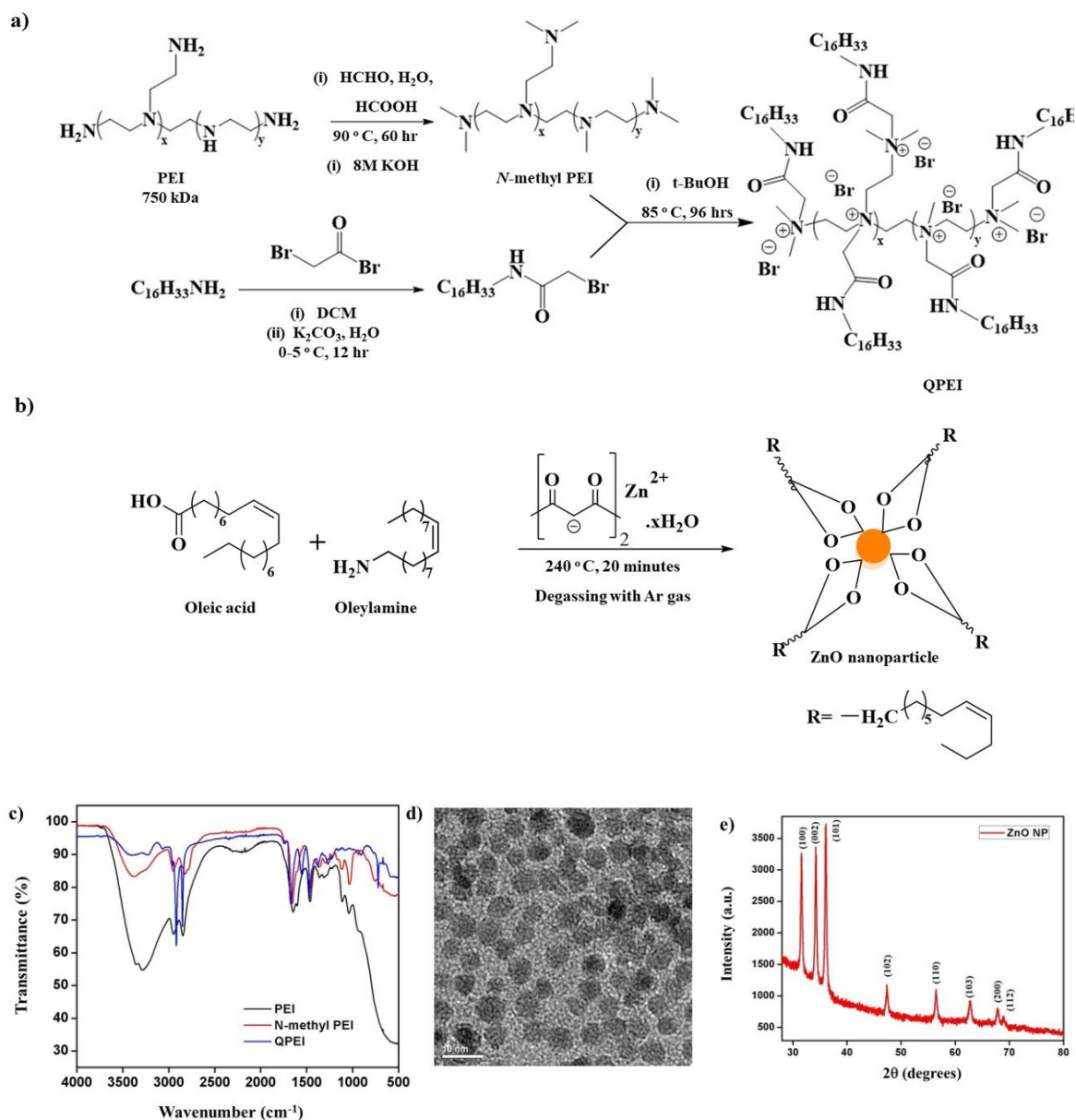


**Figure 2.1:** (a) Synthesis of branched *N*-hexadecyl-*N*-methyl PEI by *Eschweiler Clarke* methylation of branched PEI, following quaternization with alkyl bromide (b) Synthesis of zinc oxide nanoparticle from two surfactant moieties, oleyl amine and oleic acid under inert condition (c) FT-IR analysis of the synthesis of **QPEI** (d) TEM image of ZnO nanoparticles (e) XRD plot of ZnO nanoparticles showing characteristic peaks.

**2.2.2. Coating of surfaces and characterization.**  $1 \times 1 \text{ cm}^2$  silicone surfaces were coated with the 20  $\mu\text{L}$  polymer-nanocomposite solution formed by mixing polymer **QPEI** in DCM (100 mg/mL) and ZnO nanoparticles in DMSO solution (10 mg/mL) (1:1) to form (antimicrobial polymer-nanocomposite) **APN<sub>3</sub>** through drop-casting on the surfaces (Figure 2.2 a). Two other polymer-nanocomposites were also formed **APN<sub>1</sub>** (**QPEI** 50 mg/mL and ZnO 10mg/mL in DCM: DMSO solution) and **APN<sub>2</sub>** (**QPEI** 100 mg/mL and ZnO 5 mg/mL in DCM: DMSO solution). The uncoated surfaces were used as a control. SEM confirmed that the surfaces were coated, from the undulation and rough morphology observed against the smooth morphology of the uncoated silicone surfaces. Energy-dispersive X-ray confirmed from the elemental mapping the presence of nitrogen, bromine, carbon, zinc, and oxygen that the surfaces were coated with the **APN** solution the former being the elements in the **QPEI** and the latter for the nanoparticle (Figure 2.2 c-d). Bromine is the counter-ion in **QPEI**. 12 Fr silicone catheters were also cut into small pieces of length 3 cm, and dip-coated with **APN<sub>3</sub>** and characterized by FESEM (Figure 2.2 e-f) Atomic force microscopic studies further attested the uniform nature of the coating (**APN<sub>3</sub>**) with surface roughness with rms roughness of 1.94 nm (Figure 2.2 h).

**2.2.3. Visualization of Stability of Coated Surfaces through Scanning Electron Microscopy.**  $1 \times 1 \text{ cm}^2$  silicone surfaces were coated with 20  $\mu\text{L}$  **APN<sub>3</sub>** solution. The surfaces were washed in 5 cycles with water and saline to mimic the flow of urine through a catheter to check the stability of the coating, whether it washes off or not. SEM studies with elemental mapping were done. The SEM images confirmed that the coating did not wash off and

elemental mapping showed the presence of the elements of the coating. Hence, confirming the stability of the non-covalent coating on the silicone surfaces.

**2.2.4. Thermal Stability of Coating.** QPEI showed high thermal stability, as loss in weight or degradation was observed at 400 °C, showing that QPEI is a thermally stable polymer. Zinc

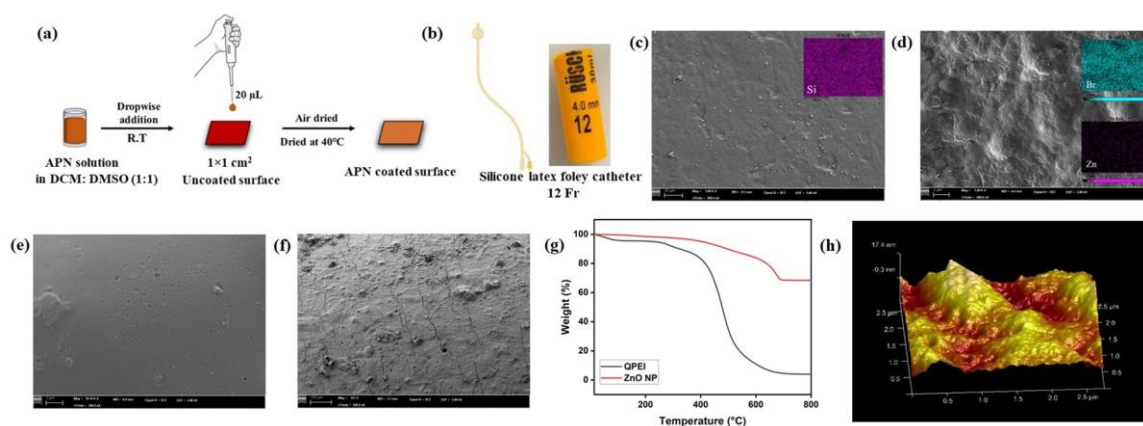


**Figure 2.2:** Surface modification and characterization of the coated surfaces (a) Schematic representation of coating of surfaces by drop-casting method (b) Cartoon image of a Foley catheter, Rusch Catheter (thickness= 12Fr) used for experiments (c-d) Scanning electron microscopy images of uncoated and APN<sub>3</sub> coated surface, respectively. The inset images represent color mapping of bromine (blue) and zinc (purple) of the coated surface after Energy dispersive X-ray analysis. Scale bar = 250 µm (e-f) Scanning electron microscopy images of uncoated and APN<sub>3</sub> coated catheter surface, respectively. (g) Thermogravimetric analysis of the stability of QPEI, and ZnO nanoparticles (h) Atomic force microscopic images of silicone surfaces coated with APN<sub>3</sub> in height phase.

oxide is capped and stabilised by oleic acid.<sup>69</sup> Degradation for the surfactant happened at a temperature of almost 650 °C proving the stability of the nanoparticle to resist melting (Figure 2.2 g). APN<sub>3</sub> hence proved the stability of the coating under thermal conditions.

**2.2.5. Antibacterial Activity of APN Coated Surfaces.** Silicone is a very commonly used material for urinary catheters. Silicone surfaces were used for the antibacterial activity of the coatings. **APN<sub>1</sub>**, **APN<sub>2</sub>**, **APN<sub>3</sub>** which constituted of different concentrations of **QPEI** and ZnO (Figure 2.3 a), were coated on 1×1 cm<sup>2</sup> silicone surfaces. It was observed that after 18 hrs of

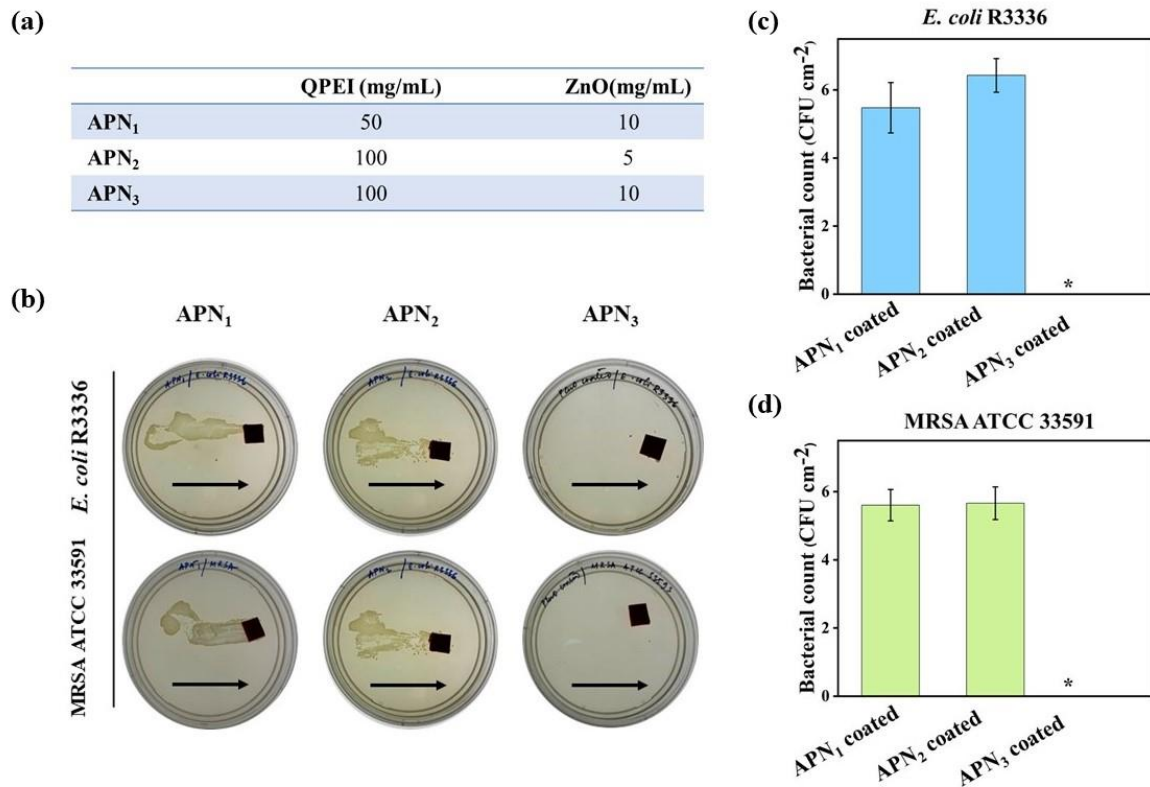


**Figure 2.3:** Antibacterial activity of different concentrations of **APN** (a) Table represents different concentrations of **QPEI** and ZnO modulated to check effective antibacterial activity (b) Antibacterial activity of **APN<sub>1</sub>**, **APN<sub>2</sub>**, and **APN<sub>3</sub>** against methicillin-resistant *S. aureus* (MRSA ATCC 33591) and *E. coli* R3336 (c-d) Reduction in bacterial count in the case of **APN<sub>3</sub>** against *E. coli* R3336 and MRSA ATCC 33591, respectively. Arrows indicate the direction of dragging of surfaces on agar plates. An asterisk (\*) indicates bacterial count of 0 CFU/mL.



incubation, **APN**<sub>1</sub>, **APN**<sub>2</sub>, had thick lawns of bacteria which grew across the agar plate. However, **APN**<sub>3</sub>, showed effective killing of MRSA ATCC 33591 and *E. coli* R3336 (Figure 2.3 b). There was ~6 log reduction in bacterial count in the case of *E. coli* R3336 and a reduction of ~5 log in the case of MRSA (Figure 2.3 c-d). Hence, for further experiments **APN**<sub>3</sub> was used.

**2.2.6. Antibacterial Activity of Coated Surfaces Against Gram-positive and Gram-negative bacteria and Counting Bacterial Reduction.** Different clinical isolates of Gram-positive bacteria *E. faecium* (VRE 903), *S. epidermidis* MTCC 3615 and MRSA ATCC 33591, the main Gram-positive bacteria causing CAUTI, along with Gram-negative bacteria *K. pneumoniae* R3934 and *K. pneumoniae* 700603 and *E. coli* R3336 were tested for antibacterial property of **APN**<sub>3</sub> coated surfaces. After the incubation period it was observed that uncoated surface, **QPEI** coated and ZnO coated surfaces showed thick growth of bacteria on agar plates however, **APN**<sub>3</sub> coated surface effectively killed all bacteria (Figure 2.4 a).

**2.2.7. Antibacterial Assay.** To quantify the killing of bacteria by **APN**<sub>3</sub> system was done by titrating the viable bacterial cells of MRSA ATCC 33591, *E. coli* R3336 and *P. aeruginosa* R590 in a plate counting method. After incubating the surfaces with bacterial cells, the surfaces were washed with saline vigorously by the rapid sonication method. The solution was diluted and plated on nutrient agar plates to let the viable cells grow. The uncoated surface showed a count of ~10<sup>4</sup> *E. coli* cells after incubation for 30 minutes whereas **APN**<sub>3</sub> showed complete killing with almost 3.8 log reduction, 4 log reduction for MRSA ATCC 33591 and in the case of *P. aeruginosa* R590 a reduction of almost 3 log (Figure 2.4 b-d). The **APN**<sub>3</sub> system shows such effective killing of a significant number of bacteria, compared to the polymer itself proves its competence to be applied on biomedical devices like urinary catheters to prevent CAUTIs.

## 2.2.8. Visualizing Antibacterial Activity of Coated Surfaces through Turbidity Test. To

validate the efficacy of bacterial killing visually, the  $APN_3$  coated surface was incubated with

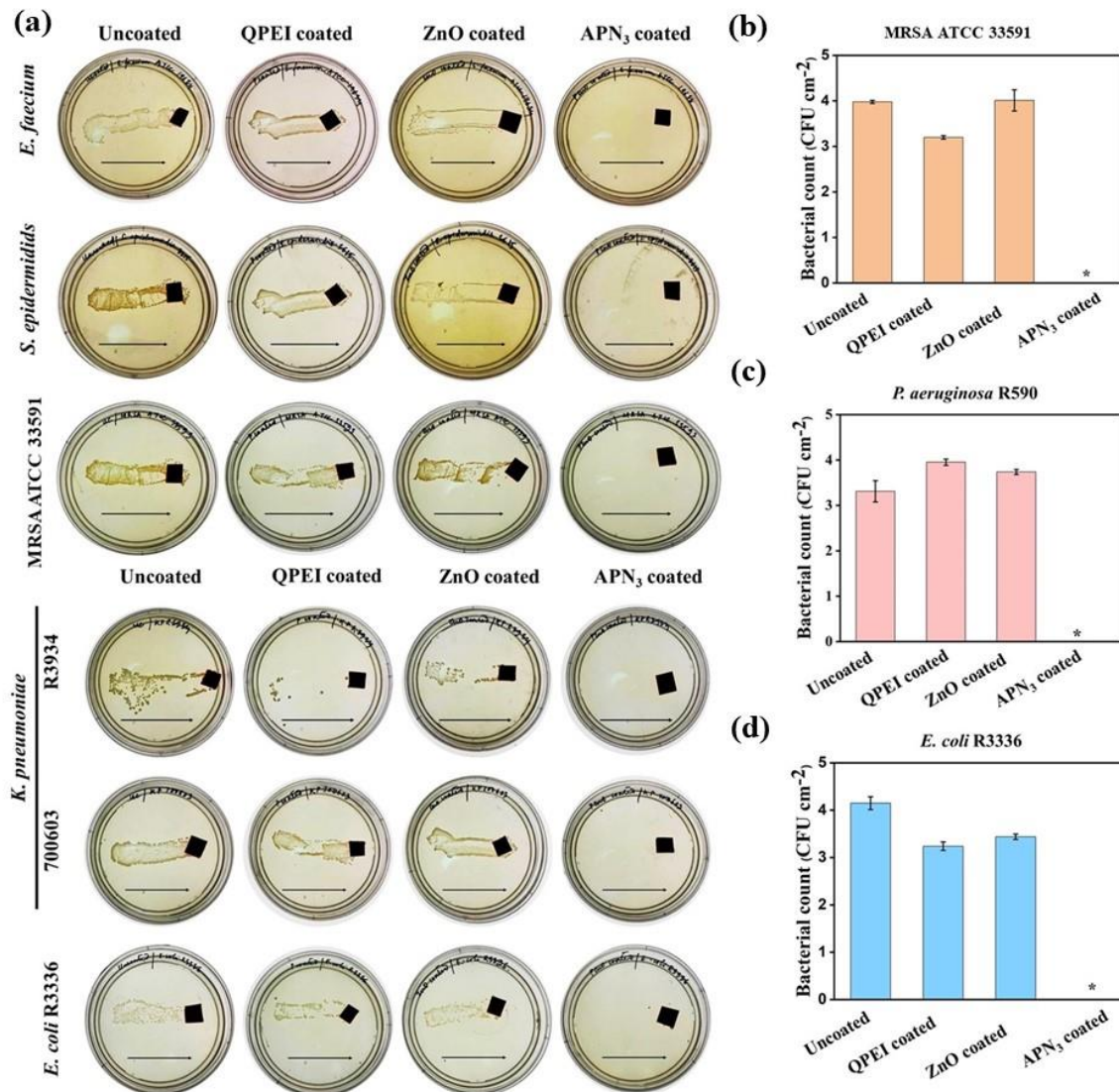


**Figure 2.4:** Effective killing of Gram-positive and Gram-negative bacteria responsible for uncomplicated and complicated UTI (a) Antibacterial activity of uncoated surface, QPEI, ZnO and  $APN_3$  coated surfaces against various Gram-positive bacteria and Gram-negative bacterial strains (b-d) Reduction in bacterial count in the case of  $APN_3$  against, MRSA ATCC 33591, *P. aeruginosa* R590 and *E. coli* R3336, respectively. Arrows indicate the direction of dragging of surfaces on agar plates. An asterisk (\*) indicates bacterial count of 0 CFU/mL.

~10<sup>6</sup> *E. coli* R3336 and *P. aeruginosa* R590 bacteria for 30 mins. After the incubation period,

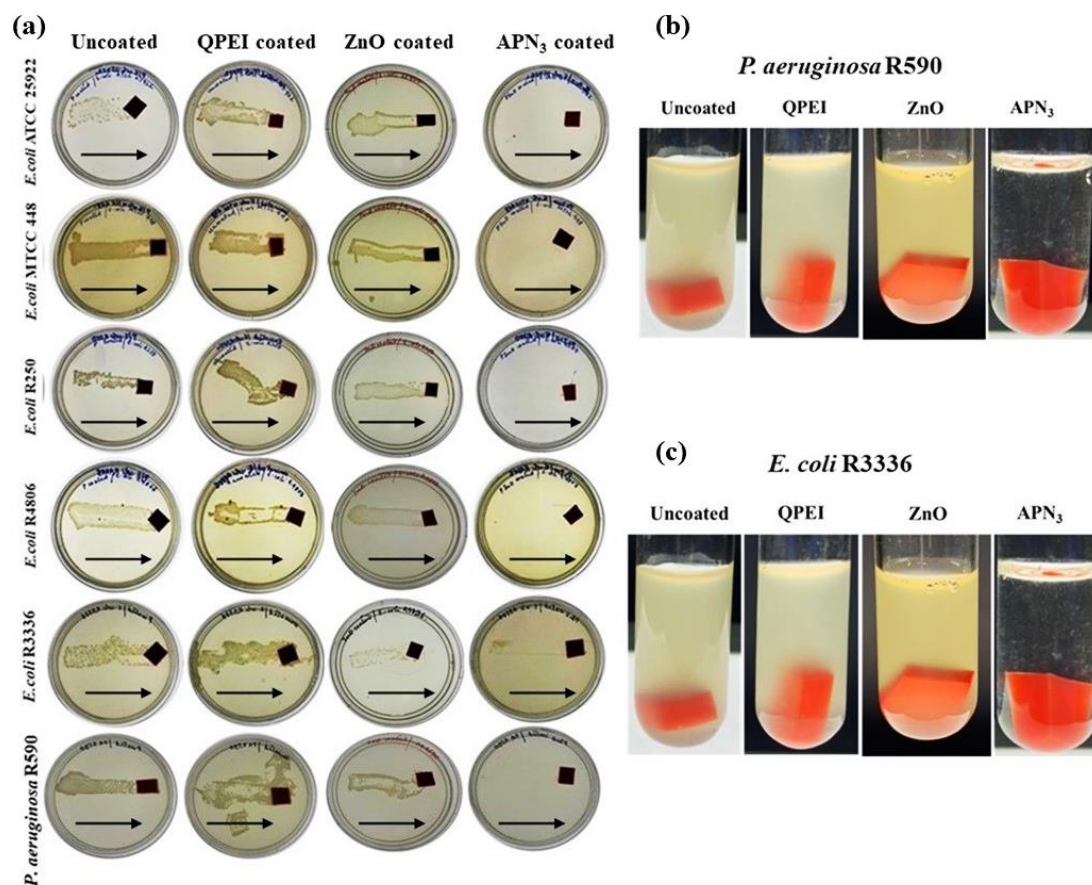


**Figure 2.5:** Potent killing of bacteria by APN<sub>3</sub> (a) Antibacterial activity of uncoated surface, QPEI, ZnO and APN<sub>3</sub> coated surfaces against various strains of *E. coli* and *P. aeruginosa* R590 by dragging across the agar plate (b-c) Visualization of antibacterial activity through turbidity test against *P. aeruginosa* R590 and *E. coli* R3336, respectively. Arrows indicate the direction of dragging of surfaces on agar plates.

the surfaces were transferred to freshly prepared growth media and allowed to grow for 18 hrs. For the uncoated surfaces, the media became turbid indicating the growth of bacteria. On the other, for polymer-nanocomposite coated surfaces, media was clear, without any turbidity, establishing the efficacy of the coating (Figure 2.5 b-c).

**2.2.9. Antibacterial Assay of Coated Surfaces by Dragging on Agar Plates. Against Planktonic Cell.** Urinary catheters are invasive medical devices that are commonly used in the treatment of urinary retention, the management of urinary incontinence, and the release of urine following genital or prostate surgery. The catheter might stay in our bodies for a short time (up to a week) or for a long time (more than four weeks), causing bacterial infections.<sup>15</sup> To ascertain the efficacy of **APN<sub>3</sub>** coated silicone surfaces, it was checked against various strains of *E. coli* and *P. aeruginosa* R590. Few of the strains were clinical isolates and even antibiotic resistant. A 20 µL bacterial suspension was dropped on the surface and incubated. After an incubation period of 30 minutes, the surfaces were dragged across the agar plate to examine the presence of live bacteria. The uncoated surface showed the growth of a thick lawn of bacterial colonies. **APN<sub>3</sub>** coated surfaces showed more effective killing than the polymer-coated silicone surfaces (Figure 2.5 a). Zinc oxide shows antibacterial properties via ROS generation, Zn<sup>2+</sup> ion generation, and electrostatic interactions.<sup>70</sup>

**Against Stationary Cell.** The prevalence of stationary bacteria cells, which remain metabolically inert and hence exceed the barrier provided by typical antibiotic therapies, is one of the alarming challenges in healthcare settings. Therefore, as a result, if antibiotic treatment is discontinued, these stationary cells may cause infections to return. The silicone surfaces coated with **APN<sub>3</sub>** showed the effective killing of live *E. coli* cells whereas uncoated surfaces showed the presence of a huge number of bacterial cells on the agar plates (Figure 2.6 a). **APN<sub>3</sub>** showed potent antibacterial activity against dormant bacterial cells, which are known to dodge the action of commercially available antibiotics.

**Against Persister Cell.** Antibiotic-resistant mutants inevitably survive, which are dormant and non-dividing cells.<sup>71</sup> *E. coli* MTCC 443 population was treated with ampicillin, and the

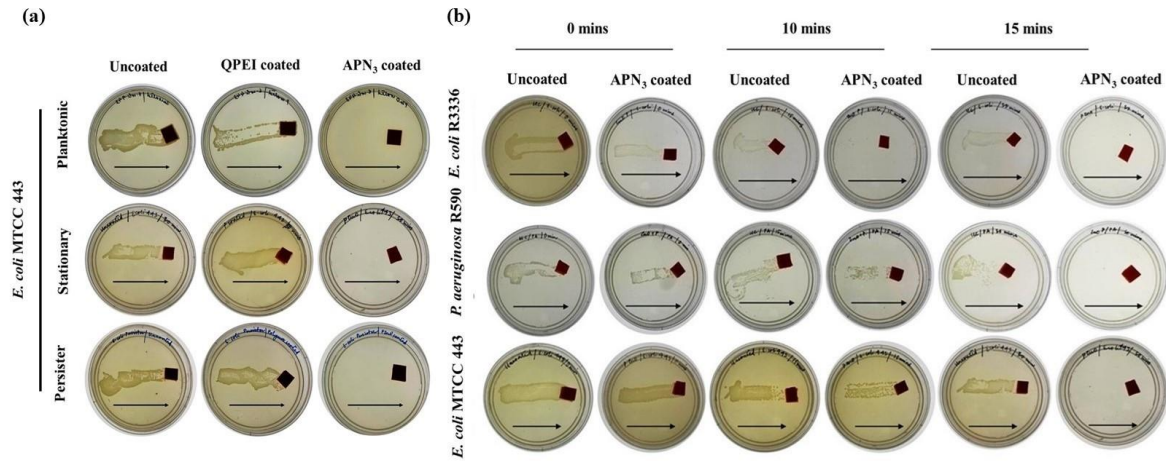


**Figure 2.6:** Rapid antibacterial activity (a) Antibacterial activity of uncoated surface, QPEI and APN<sub>3</sub> coated surfaces against planktonic-phase, stationary-phase and persister-phase cells of *E. coli* MTCC 443 by dragging across the agar plate (b) Bactericidal kinetics of uncoated and APN<sub>3</sub> coated surfaces against *E. coli* R3336, *P. aeruginosa* R590 and *E. coli* MTCC 443, respectively. Arrows indicate the direction of dragging of surfaces on agar plates.

surviving cells were allowed to grow which gave rise to antibiotic-resistant *E. coli* strain which commonly leads to recurrent UTI. Recurrent UTI is highly prevalent and accounts for the leading cause of hospital-acquired infections and the subsequent morbidity.<sup>72</sup> APN<sub>3</sub> coated surfaces showed the effective killing of notorious, antibiotic-resistant *E. coli* strain within 30-40 minutes with no growth of bacterial lawn across the agar plate (Figure 2.6 a). Uncoated and polymer-coated surfaces showed thick growth of the bacterial colony, hence proving the efficacy of our coating is killing bacterial cells by not only targeting metabolically active cells but also through membrane disintegration by disrupting the cell envelope.

**2.2.10. Bactericidal Kinetics.** Bacterial colonization on invasive biomedical devices can cause major life-threatening infections. Infections through catheters can spread during the handling of the catheters so it is important for surfaces to rapidly kill bacterial cells before the infection

prevails. To evaluate how fast bacterial cells can be eradicated, bactericidal kinetics was performed for the silicone surfaces coated with **APN<sub>3</sub>**. Upon incubation of these surfaces with *E. coli* R3336, *E. coli* MTCC 443, and *P. aeruginosa* R590 stationary cells, the surfaces showed effective killing within 15-30 minutes. The coating killed viable planktonic *E. coli* R3336 bacterial cells within 10 mins (Figure 2.6 b). This showed that the coating has outstanding killing rates, making them a suitable candidate for antimicrobial applications.

**2.2.11. Antibacterial Activity of Urinary Catheters.** To mimic the actual situation of a urinary catheter being infected with bacteria during its handling or implantation, a 12 Fr urinary catheter was cut into pieces and incubated with Gram-negative *E. coli* R3336, one of the main pathogens leading to UTIs. When incubated and dragged across the agar plate, a thick lawn of bacteria grew for the uncoated catheters and no bacterial colonies were observed in the case of **APN<sub>3</sub>** coated catheters proving to be an effective candidate against catheter-associated urinary tract infections with a ~5.8 log reduction in *E. coli* R3336 bacterial cells (Figure 2.7 a,c).

**2.2.12. Repeated Antibacterial Activity of Coated Surfaces.** Sometimes, on repeated usage of catheters because of washing off the coating can lead to the diminution of the efficacy of the catheters leading to infections. To understand this, in small scale, the surfaces were washed in 3 cycles for 1 minute each with 1 mL saline and water. After washing, the surfaces were incubated with *E. coli* R3336 and *E. coli* MTCC 443 for 45 minutes. Once dragged across the agar plate, and incubated at 37 °C for 18 hrs, the uncoated control surfaces showed thick bacterial colonies whereas the **APN<sub>3</sub>** coated surfaces showed no growth in bacterial colonies with ~6 log reduction against *E. coli* MTCC 443. Even though the surfaces took a little more time in killing<sup>73</sup> the bacteria than an unwashed coated catheter surfaces that shows effective

killing in 10-15 minutes, the washed surfaces also was equally effective in killing bacteria rapidly (Figure 2.7 b,d).

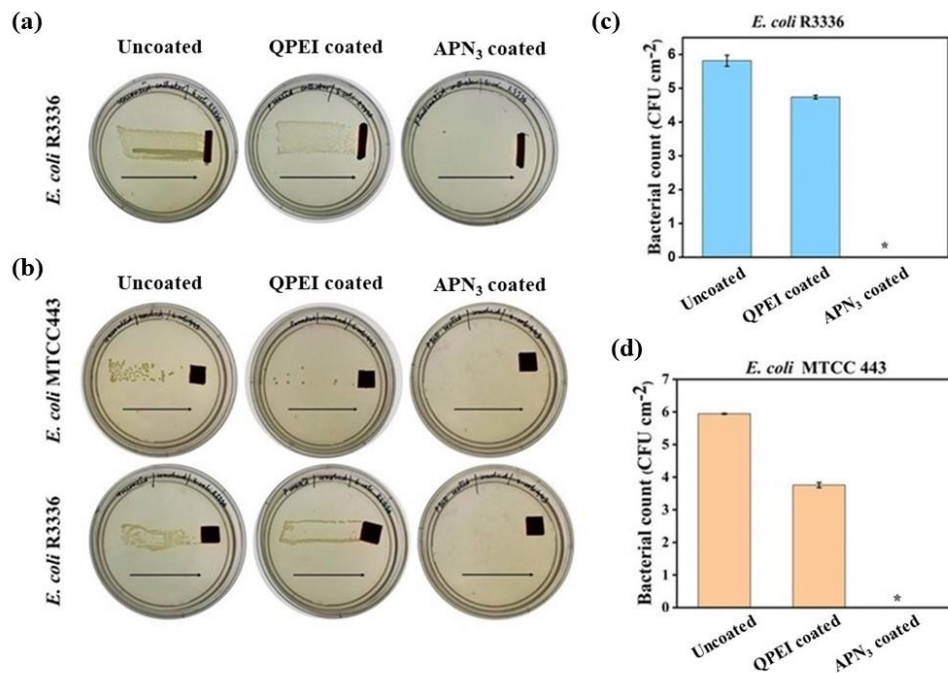


**Figure 2.7:** Retainment of antibacterial activity of coated surfaces (a) Antibacterial activity of uncoated surface, **QPEI** and **APN<sub>3</sub>** coated catheter surfaces against *E. coli* R3336 by dragging across the agar plate (b) Antibacterial activity of uncoated, **QPEI** and **APN<sub>3</sub>** coated silicone surfaces after washing the surfaces with saline and water. Arrows indicate the direction of dragging of surfaces on agar plates. An asterisk (\*) indicates bacterial count of 0 CFU/mL.

**2.2.13. Bacterial Biofilm Inhibition Study.** In clinical settings, bacterial biofilm formation is one of the most prevalent causes of severe and chronic illnesses. Biofilm is a multicellular microbial structure composed of a self-produced extracellular matrix, antimicrobial diffusion barriers, and many metabolically inactive or dormant bacterial cells. Furthermore, planktonic and biofilm embedded bacterial cells were revealed to be different than dispersed cells resulting from mature biofilm dispersion.<sup>73</sup> So, next the bacterial biofilm inhibition was checked for the **APN** system against *E. coli* R3336, *E. coli* MTCC 443 and MRSA ATCC 33591. The biofilm

formation was visually imaged via CLSM imaging after staining with SYTO 9 and PI.

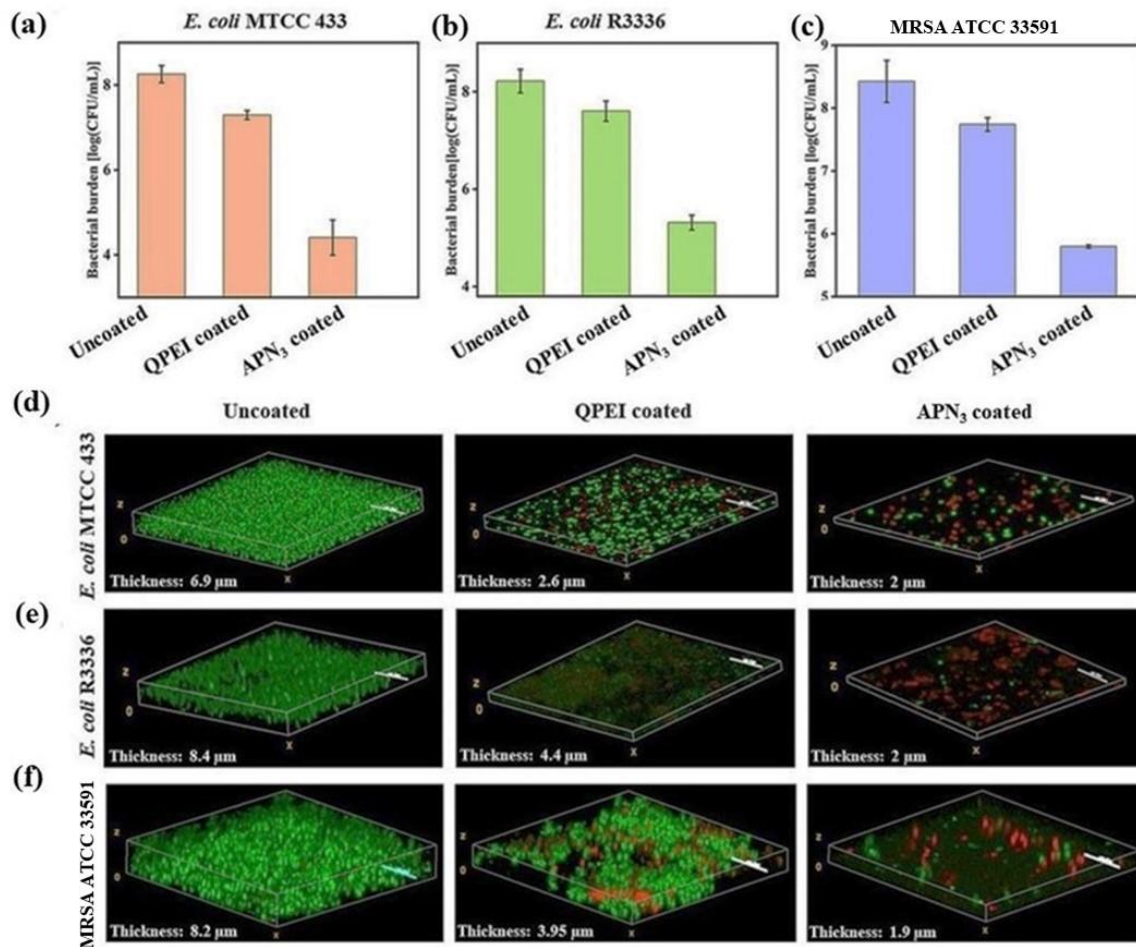


**Figure 2.8:** Biofilm inhibition study (a-c) Reduction in bacterial burden in *E. coli* MTCC 443, *E. coli* R3336 and MRSA ATCC 33591 biofilm (d-f) CLSM images of biofilm formation in uncoated, QPEI and APN<sub>3</sub> coated surfaces. Scale bar = 10 μm.

Uncoated coverslips showed colossal growth of bacterial biofilm of thickness 8.4 μm, 6.9 μm and 8.2 μm for *E. coli* R3336, *E. coli* MTCC 443 and MRSA ATCC 33591 respectively, both grown for 72 hrs (Figure 2.8 d-f). On the other hand, APN<sub>3</sub> coated coverslips showed a thickness of 2 μm proving the efficacy to inhibit the growth of biofilm on the surfaces. To quantify the biofilm biomass grown, the surfaces were washed with saline and Trypsin-EDTA. The solution was diluted and plated on agar plates. The coated surfaces showed a 4 log



reduction in cell viability in the case of *E. coli* MTCC 443 and a 3 log reduction for *E. coli* R3336 indicating the potential of **APN<sub>3</sub>** in inhibiting bacterial colonization onto the surfaces (Figure 2.8 a-c).

**2.2.14. Antifungal Assay of Coated Surfaces by Dragging on YPD Plates.** *Candida* species are commonly found in the human gastrointestinal system, vaginal tract, and skin.<sup>72</sup> During their stay in the hospital, patients, particularly those in the intensive care unit (ICU), accumulate several risk factors, and candiduria is a regular occurrence leading to fungal UTI. *Candida* species account for 78.3% of nosocomial fungal infections. Hence, the efficacy of the coating was checked against fluconazole-resistant, *C. albicans* AB226, and *C. albicans* AB399. A 20  $\mu$ L fungal suspension was dropped on the surface and incubated. The **APN<sub>3</sub>** coated surfaces when dragged across YPD agar plates showed no fungal growth whereas uncoated surfaces showed thick lawns of fungi on the plate (Figure 2.9 a). The coating showed effective 100 % killing of the fungal strains within 1-2 hours proving its superior potency against deadly fungal strains.

**2.2.15. Antifungal Assay.** To quantify the antifungal activity of the coated and uncoated surfaces were incubated with viable fungal cells of *C. albicans* AB226 and *C. albicans* AB399. The surfaces were washed with saline and the solution was tittered and plated for counting of fungal colonies. After an incubation period of 2 hrs, **APN<sub>3</sub>** coated surfaces showed a 4 log reduction for both *C. albicans* strains whereas the uncoated surfaces showed  $\sim 10^4$  fungal cells (Figure 2.9 b,d).

**2.2.16. Fungicidal Kinetics.** It is important to measure how rapidly the **APN<sub>3</sub>** coating can eradicate fungal strains. Upon incubation of the surfaces at different time points, 0 minutes, 30 minutes, 1 hr, and 2 hrs with *C. albicans* AB226 and *C. albicans* AB399. The coating effectively killed *C. albicans* AB226 within an hour whereas *C. albicans* AB399 took 2 hrs to

get killed. Within 1-2 hrs, the coating killed 100 % of the fungal strains, demonstrating its higher effectiveness against lethal fungal strains (Figure 2.9 c).

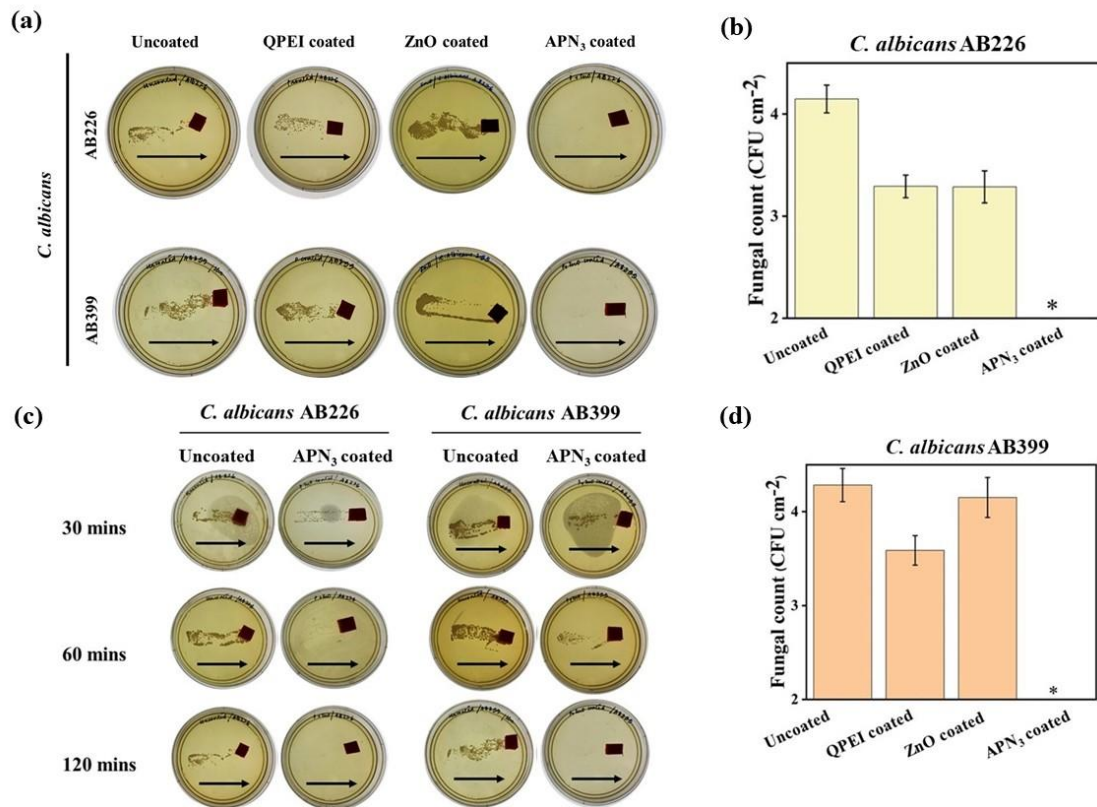


**Figure 2.9:** Antifungal study (a) Antifungal activity of uncoated, QPEI, ZnO and APN<sub>3</sub> coated surface against *C. albicans* AB226 and *C. albicans* AB399 (b,d) Reduction in fungal count against *C. albicans* AB226 and *C. albicans* AB399 (c) Fungicidal kinetics of uncoated and APN<sub>3</sub> coated surfaces. Arrows indicate the direction of dragging of surfaces on YPD agar plates. An asterisk (\*) indicates fungal count of 0 CFU/mL.

**2.2.17. Visualization of Antibacterial Activity of Coated Surfaces through Scanning Electron Microscopy.** To have a better understanding of the killing of bacteria by APN<sub>3</sub>, the bacterial morphology of *E. coli* MTCC 443 was visualized by scanning electron microscopy after incubation with coated polystyrene surfaces. The images of the cells incubated in the uncoated wells showed the retention of well-defined morphology and rod-shaped *E. coli*

bacteria. Whereas, coated wells showed the disruption of the bacterial cells, indicating loss of structural integrity of the bacterial cells along with debris observed, affirming membrane disruption (Figure 2.10 b-c).

**2.2.18. Live-Dead Assay of the Coating Against Bacteria.** To visualize the membrane disruption of the bacteria, Live-Dead assay was done. 100  $\mu$ L of *E. coli* MTCC 443 were dropped into 10 wells and incubated for 1 hr. Fluorescence imaging of living and dead bacterial cells was done using SYTO-9 and PI dyes to see how the coating killed the bacteria. The appearance of green fluorescence validated that practically all bacteria were alive. Observation of the merged green and red fluorescence from SYTO-9 and PI staining indicated the presence of dead bacteria when the well plates were coated (Figure 2.10 d).

**2.2.19. Flow cytometric analysis of intracellular ROS.** To fight excessive ROS generation, the cell has a robust antioxidant defence mechanism. When the production of reactive oxygen species (ROS) outnumbers the cells' natural antioxidant defences, oxidative stress ensues.<sup>74</sup> DCF, a membrane permeable oxidised fluorescent result of DCFH<sub>2</sub>, can leak out of cells over time signalling the generation of ROS.<sup>75</sup> Uncoated surface showed no ROS generation as predicted, whereas **QPEI** coated surface showed a very low percentage of ROS generation. ZnO having an inherent property of generating ROS showed a percentage of 2.1% of intracellular ROS generation in 10 mins. However, polymer-nanocomposite system, **APN<sub>3</sub>**, due to the synergistic effect of polymer and metal oxide nanoparticle showed high amount of ROS generation amounting to 50.3% to kill the bacterial cells in the 10 minutes. ROS generation being one of the main reasons for the rapid antibacterial activity showed by **APN<sub>3</sub>** coated surfaces (Figure 2.10 a).

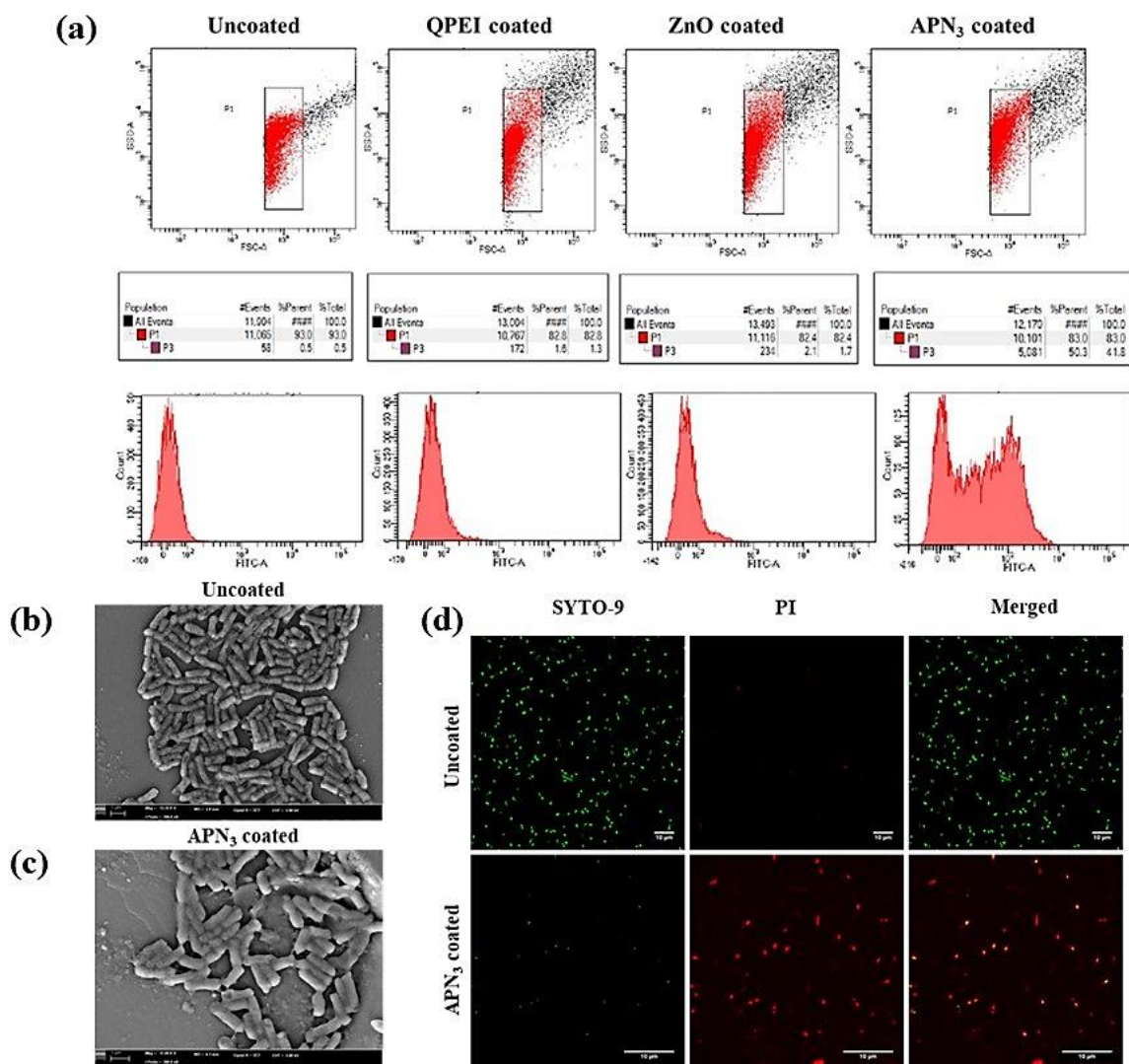


**Figure 2.10:** Membrane-active property of APN<sub>3</sub> coating (a) Flow cytometric analysis of intracellular ROS by uncoated surface, QPEI, ZnO and APN<sub>3</sub> coated surfaces (b-c) Observation of bacterial killing through scanning electron images of *E. coli* MTCC 443 (d) Live-Dead assay images of bacterial killing. Scale bar = 10  $\mu$ m.

### 2.3. Conclusion

In this study we have developed a non-covalent-based polymer nanocomposite (**APN<sub>3</sub>**) coating with an organo-soluble, hydrophobic quaternized polyethyleneimine (**QPEI**) backbone functionalized with a hexadecyl amide long chain typically for urinary catheter surfaces like silicone integrated with zinc oxide nanoparticles that showed effective killing of both Gram-positive and Gram-negative bacteria responsible for CAUTIs. Our polymer-nanocomposite showed antibacterial activity via membrane disruption and rapid ROS generation. It is evident that encrustation of catheter surfaces due to biofilms are a menace, which was also tackled by the coated surface inhibiting its growth. In addition to these, one of the other highlights of our system is to combat yeast infections that are usually accompanied with the bacterial infections during catheterization for a long period of time. Altogether, the overall results suggest that the **APN<sub>3</sub>** coating bears an immense potential in eradicating catheter-associated urinary tract infections.

### 2.4. Materials and methods

Spectrochem provided reagent grade chloroform (CHCl<sub>3</sub>), dichloromethane (DCM), ethanol (EtOH), tert-butanol (tBuOH), and methanol (MeOH) (India). Isopropanol (IPA) of HPLC quality was obtained from Spectrochem. Sigma Aldrich provided dimethyl sulphoxide (DMSO) and poly(2-ethyl-2-oxazoline). Wherever solvents needed to be dried, it was done. Sigma Aldrich provided the 1-hexadecane. The chemicals were employed in the process directly. Nuclear magnetic resonance (NMR) spectra of the compounds were recorded in deuterated solvents in a Bruker AMX-400 spectrometer. A local hardware store provided silicone sheets with a thickness of 0.7 mm. *E. coli* R3336, *E. coli* MTCC 443, *E. coli* ATCC 25922, *E. coli* MTCC 448, *E. coli* R250, *E. coli* 4806, and *P. aeruginosa* R590, MRSA ATCC

33591, *E. faecium* ATCC 19634, *S. epidermidis* 3615, *K. pneumoniae* R3934, and *K. pneumoniae* 700603 were obtained from the National Institute of Mental Health and Neurosciences (NIMHANS), Bangalore, India. Fungal strains (*C. albicans* AB226 and *C. albicans* AB399) were obtained from Anthem Biosciences, Bangalore, India. As a solid growth medium, nutrient agar was used for both Gram-negative and Gram-positive bacteria. YPD agar was used for fungi-related experiments. The 96-well plates and 6-well plates were obtained from Tarsons (India). SEM and EDX were performed in Zeiss Gemini 500 FESEM comprising an EDX unit. Confocal studies were performed in Zeiss LSM 800. Thermogravimetric analysis (TGA) was performed on the Perkin Elmer STA 6000. FACS studies were performed on BD FACSAria III.

## 2.5. Experimental section

### 2.5.1. Synthetic protocol

#### 2.5.1.1. Synthesis of *N*-hexadecyl-2-bromoethanamide

In DCM (55 mL), 1-aminohexadecane (64 mmol) was added, followed by an aqueous solution of  $K_2CO_3$  (95 mmol) (60 mL). After that, the mixture was cooled to 5 °C. Bromoacetyl bromide (95 mmol) dissolved in anhydrous DCM (55 mL) and was added dropwise to the mixture over 30 minutes. The reaction was then allowed to continue at room temperature (RT). The DCM layer was collected using a separating funnel after 18 hrs. DCM (250 mL) was used to wash the remaining aqueous layer. The DCM solutions were then combined and washed three times with water (100 mL each time). Finally, the DCM layer was washed with anhydrous sodium sulphate ( $Na_2SO_4$ ) and removed with a rotary evaporator to yield a colourless solid.

***N*-hexadecyl-1-bromoethanamide:** FT-IR ( $\nu$ ): 3252  $cm^{-1}$  (amide N–H str.), 2925  $cm^{-1}$  (–CH<sub>2</sub>– assym. str.), 2850 (–CH<sub>2</sub>– sym. str.), 1679  $cm^{-1}$  (Amide I, C=O str.), 1565  $cm^{-1}$  (Amide II, N–H ben.), 1469  $cm^{-1}$  (–CH<sub>2</sub>– scissor); <sup>1</sup>H-NMR: (400 MHz,  $CDCl_3$ ):  $\delta$  0.87 (t, terminal–CH<sub>3</sub>,

3H), 1.310 (m,  $-(\text{CH}_2)_{13}-$ , 26H), 1.550 (q,  $-\text{CH}_2(\text{CH}_2)_{13}-$ , 2H), 3.278 (t,  $-\text{CONHCH}_2-$ , 2H), 3.880 (s,  $-\text{COCH}_2\text{Br}$ , 2H), 6.572 (br s, amide  $-\text{NHCO}$ , 2H).

### 2.5.1.2. Synthesis of *N*-Methyl branched PEIs

Polyethyleneimine (PEI) (750kDa) (5.6 g) was taken in a round-bottom flask and formic acid (3.4 mL) was added followed by the addition of formaldehyde (5.45 mL) and 20 mL of water. The reaction mixture was stirred at 90 °C for 60 hrs. The reaction mixture was cooled to room temperature after which KOH (8M) solution was added to the reaction mixture until the pH was ~11. The organic solution was subjected to repeated chloroform wash. The obtained product after removing chloroform had a 100% degree of methylation.

***N*-Methyl branched PEI:** FT-IR ( $\nu$ ): 2947 and 2785  $\text{cm}^{-1}$  (C-H str), 1463  $\text{cm}^{-1}$  (C-H bend), 1030  $\text{cm}^{-1}$  (C-N str);  $^1\text{H}$  NMR (400 MHz,  $\text{CDCl}_3$ ,  $\delta$ ): 2.250 (s, 3H,  $-\text{N}(\text{CH}_3)-$ ), 2.426-2.605 (m, 4H,  $-\text{N}(\text{CH}_2\text{CH}_2)-$ ).

### 2.5.1.3. Synthesis of *N*-hexadecyl, *N*-Methyl PEIs

Methylated PEI (17.5 mmol/repeating unit) was reacted directly with *N*-hexadecyl-2-bromoethanamide (26.3 mmol) after dissolving it in tert-butanol (50 mL) in a pressure tube for 96 hrs at 75 °C. The resulting reaction mixture was concentrated using the rotary evaporator. Then, an excess of diethyl ether was used to obtain a pale-brown product for purification. The excess of diethyl ether was decanted, and any unwanted solvent was removed by drying the precipitate in a high vacuum pump to obtain the quaternized PEI (**QPEI**).

***N*-hexadecyl, *N*-Methyl PEI:** FT-IR ( $\nu$ ): 3200-3450  $\text{cm}^{-1}$  (amide N-H str.), 2935  $\text{cm}^{-1}$  ( $-\text{CH}_2-$  assym. str.), 2865  $\text{cm}^{-1}$  ( $-\text{CH}_2-$  sym. str.), 1680  $\text{cm}^{-1}$  (amide I, C=O str.), 1556  $\text{cm}^{-1}$  (amide II, N-H ben.), 1475  $\text{cm}^{-1}$  ( $-\text{CH}_2-$  scissor);  $^1\text{H}$ -NMR (400 MHz,  $\text{CDCl}_3$ ,  $\delta$ ): 0.856 (t, terminal  $-\text{CH}_3$ , 3H), 1.233 ( $-\text{CH}_3(\text{CH}_2)_{13}\text{CH}_2-$ , 26H), 1.510 ( $\text{CH}_3(\text{CH}_2)_{13}\text{CH}_2\text{CH}_2-$ , 2H), 3.186 ( $-(\text{CH}_3)\text{N}^+(\text{CH}_2\text{CH}_2)_2(\text{CH}_2\text{CONH})-$ , 3H), 3.480-3.585 ( $-(\text{CH}_3)\text{N}^+(\text{CH}_2\text{CH}_2)_2(\text{CH}_2\text{CONH})-$ ,

4H), 3.835 ( $-\text{CH}_2\text{CONHCH}_2\text{CH}_2-$ , 2H), 4.475 ( $-(\text{CH}_3)\text{N}^+(\text{CH}_2\text{CH}_2)_2(\text{CH}_2\text{CONH})-$ , 2H), 8.320 ( $-\text{CH}_2\text{CONHCH}_2\text{CH}_2-$ , 1H)

#### 2.5.1.4. Synthesis of ZnO nanoparticles

Zinc oxide nanoparticles (ZnO NP) were synthesized using zinc acetylacetonate monohydrate (6 mmol) as a metal precursor in the presence of two surfactants, namely oleyl amine (18 mmol) and oleic acid (3.6 mmol).<sup>69</sup> The resulting mixture was first degassed and then heated in an argon flux. To allow for the growth of the ZnO NP, the synthesis was carried out at 240 °C for 20 minutes under argon flow. After cooling, the resulting nanocrystalline product was precipitated from the reaction mixture using absolute ethanol. To remove any precursor and surfactant residuals, the product was centrifuged and thoroughly purified through repeated cycles of dispersion in chloroform and reprecipitation with absolute ethanol. Because of their hydrophobic organic coating, the final NP showed good dispersibility in chloroform. A white powder was obtained after air drying for X-ray diffraction, Transmission Electron Microscopy (TEM), and FT-IR.

*X-ray Diffraction (XRD).* Zinc oxide (ZnO) nanoparticles were dispersed in chloroform (10 mg/mL) and drop-casted on a  $2 \times 2 \text{ cm}^2$  glass slide. On air-drying, the sample was used for XRD measurements.

*Transmission Electron Microscopy (TEM).* Zinc oxide nanoparticles were dispersed in chloroform (0.2 mg/mL) and drop-casted on a TEM grid and the images were captured in JEOL JEM 2100 Plus operating at an acceleration of 200 kV.

*FT-IR.* The dried ZnO nanoparticle sample was directly used for FT-IR measurements.



### 2.5.1.5. Coating of surfaces and characterization

100 mg/mL **QPEI** solution in DCM and a 10 mg/mL solution of zinc oxide in DMSO were prepared and mixed (1:1) to obtain the antimicrobial polymer nanocomposite (**APN**). Silicone surfaces to mimic the catheter surface were cut into  $1 \times 1 \text{ cm}^2$  pieces and washed in three cycles with isopropanol and further with water and acetone to remove any unwanted impurities. After the surfaces were dried, 20  $\mu\text{L}$  of the organo-solution was drop-casted on the surfaces and dried at room temperature and then  $40 \text{ }^\circ\text{C}$ . The surface morphology was determined through Field-emission scanning electron microscopy (FESEM), Energy dispersion X-ray (EDX), and atomic force microscopy (AFM). 12 Fr silicone catheters were cut into small pieces of length 3 cm, and dip-coated with **APN** and characterized by FESEM.

*Field Emission Scanning Electron Microscopy (FESEM).* Uncoated, polymer (**QPEI**) coated, and **APN** coated surfaces were characterized by FESEM studies with gold-sputtering before imaging.

*Energy dispersive X-ray (EDX).* EDX analysis of the silicone samples was done using the Zeiss Gemini 500 FESEM instrument holding the EDX unit. Gold-sputtering was done before sample analysis.

*Atomic Force Microscopy (AFM).* AFM measurements of the silicone-coated and uncoated surfaces were performed on the Bruker Innova AFM using a cantilever made of silicon in tapping mode with frequency, in the range of 300 and 400 kHz and a spring constant value of  $40\text{-}80 \text{ Nm}^{-1}$ .

**2.5.1.6. Visualization of Stability of Coated Surfaces through Scanning Electron Microscopy.**  $1 \times 1 \text{ cm}^2$  silicone surfaces and catheter surfaces were coated through drop-casting and dipping-method with the **APN** solution. The surfaces were washed in 5 cycles with saline

and water. The washed surfaces were then characterized by scanning electron microscopy and energy-dispersive X-ray with gold sputtering before imaging.

**2.5.1.7. Thermal Stability of Coating.** QPEI and Zinc oxide nanoparticles were checked for thermal stability through Thermogravimetric analysis (TGA) on the Perkin Elmer STA 6000.

## **2.5.2. Biological Assays**

**2.5.2.1. Antibacterial Activity of APN Coated Surfaces.** Different concentrations of APN were taken to check the initial antibacterial activity. Three systems were developed APN<sub>1</sub>, APN<sub>2</sub>, APN<sub>3</sub>, were taken and 20 µL of the solutions were drop-casted on silicone. Gram-positive MRSA ATCC 33591 and *E. coli* R3336 were cultured at 37 °C for 6 hrs in a nutrient media under constant shaking condition. The bacterial solution was diluted to a suspension of 10<sup>6</sup> CFU/mL in saline. 20 L of the solution was poured onto the coated surfaces and incubated for 30 minutes at 37 °C. Finally, the silicone surfaces were dragged across the nutrient agar plate along its diameter and incubated for 18 hours. Similarly, the surfaces were rinsed with 990 L saline after incubation. After serial dilution, 20 litres of the solutions were dropped onto nutrient agar plates. The agar plates were incubated for 18 hrs at 37 °C, after which the bacterial colonies were counted.

**2.5.2.2. Antibacterial Activity of Coated Surfaces by Dragging on Agar Plates Against Gram-positive and Gram-negative bacteria and Counting Bacterial Reduction.** Different clinical isolates of Gram-positive bacteria *E. faecium* (VRE 903), *S. epidermidis* MTCC 3615 and MRSA ATCC 33591, the main Gram-positive bacteria causing CAUTI, along with Gram-negative bacteria *K. pneumoniae* R3934 and *K. pneumoniae* 700603 and *E. coli* R3336. The bacteria were cultured at 37 °C for 6 hrs in a nutrient media under constant shaking condition. *E. faecium* was cultured in brain heart infusion (BHI) media under same conditions. The bacterial solution was diluted to ~10<sup>6</sup> CFU/mL suspension in saline. 20 µL of this bacterial

suspension was dropped on the 1×1 cm<sup>2</sup> surfaces of silicone coated with **QPEI**, ZnO and **APN<sub>3</sub>**. In the experiment, the uncoated silicone surfaces were used as the control. The surfaces were then covered with a coverslip to spread the bacterial suspension homogeneously over the surfaces. After incubation at 37 °C for 30 minutes, the silicone surfaces were dragged across the nutrient agar plate along its diameter. The plates were then incubated at 37 °C for 18 hrs followed by imaging of these plates.

**2.5.2.3. Antibacterial Assay.** The antibacterial assay of the **APN<sub>3</sub>** and **QPEI** coated silicone surfaces was done using the previously reported protocol.<sup>68</sup> Pristine surfaces were used as the control for the experiment. 20 μL of ~10<sup>6</sup> CFU/mL bacterial suspension of MRSA ATCC 33591, *E. coli* R3336 and *P. aeruginosa* R590 was dropped on 1×1 cm<sup>2</sup> coated and uncoated surfaces and covered with a coverslip and incubated at 37 °C for 30 minutes. Post-incubation the surfaces were washed with 990 μL saline. Serial dilution was conducted and 20 μL of the solutions were drop-casted on nutrient agar plates. The agar plates were incubated for 18 hrs at 37 °C, consequently counting the bacterial colonies.

**2.5.2.4. Visualization of Antibacterial Activity of Coated Surfaces through Turbidity Test.** *E. coli* R3336 and *P. aeruginosa* R590 were made to grow in a suitable nutrient media for 6 hours under continuous shaking conditions. The bacterial suspension was diluted to ~10<sup>6</sup> CFU/mL in saline. **QPEI** and **APN<sub>3</sub>** coated 1×1 cm<sup>2</sup> surface was dropped into these bacterial solutions and incubated at 37 °C for 2 hrs. The uncoated surfaces were treated as the control for the experiment. The surfaces were then dropped into freshly prepared nutrient media (5 mL) and incubated at 37 °C for 18 hrs. After the incubation period, the tubes were investigated visually, and their photographs were captured.

**2.5.2.5. Antibacterial Assay of Coated Surfaces by Dragging on Agar Plates. Against Planktonic Cell.** Different clinical-isolates and drug-resistant strains of *E. coli* (*E. coli* R3336,

*E. coli* MTCC 443, *E. coli* ATCC 25922, *E. coli* MTCC 448, *E. coli* R250, *E. coli* 4806) and *P. aeruginosa* R590 were grown at 37 °C for 6 hrs in a nutrient media under constant shaking condition. The bacterial solution was then diluted to prepare a  $\sim 10^6$  CFU/mL suspension in saline. An aliquot of 20  $\mu$ L of this bacterial suspension was dropped on the  $1 \times 1$  cm<sup>2</sup> surfaces of silicone coated with **QPEI** and **APN<sub>3</sub>**. The rest of the experiment was done similar to the previously conducted experiment.

**Against Stationary Cell.** A stationary-phase *E. coli* MTCC 443 culture was created by diluting a mid-log phase bacterial culture 1000 times in nutrient broth and incubating it at 37 °C for 16 hrs under shaking conditions. After which the bacterial suspension was centrifuged (9000 rpm, 3 minutes) and was resuspended in saline. The suspension was diluted in saline to a concentration of  $\sim 10^5$  CFU/mL, which was used in the experiment. The protocol after this is like the bacterial assay against planktonic cells that have been described earlier.

**Against Persister Cell.** Initial steps to culture and dilute a mid-log phase bacterial suspension of *E. coli* MTCC 443 are like that described earlier in the bacterial assay against stationary cells. After centrifugation (9000 rpm, 3 minutes) the bacterial precipitate was treated with 300  $\mu$ g/mL Ampicillin solution. The suspension was incubated at 37 °C for 4 hrs under shaking conditions. After which the bacterial solution was again centrifuged (9000 rpm, 3 minutes) and resuspended in saline. The suspension was diluted in saline to a concentration of  $\sim 10^5$  CFU/mL, which was used in the experiment. The protocol after this is like the bacterial assay against planktonic cells that have been described earlier.

**2.5.2.6. Bactericidal kinetics.** A bacterial culture of *E. coli* R3336 ( $\sim 10^6$  CFU/mL) was diluted from a mid-log phase ( $\sim 10^8$  CFU/mL) in saline solution from a mid-log phase ( $\sim 10^8$  CFU/mL) in saline solution. An aliquot of 20  $\mu$ L of this bacterial solution was dropped on  $1 \times 1$  cm<sup>2</sup> silicone coated with **QPEI** and **APN<sub>3</sub>**. The uncoated silicone surfaces were employed as the

control in the experiment. After that, the surfaces were covered with a coverslip to evenly distribute the bacterial suspension. The samples were incubated for different time points such as 0, 5, 10, 15, 30, 45 mins at 37 °C. These surfaces were then dragged across the nutrient agar plates along the diameter of the plate and incubated at 37 °C for 18 hrs followed by taking photographs of the plates.

**2.5.2.7. Antibacterial Activity of Urinary Catheters.** A 12 Fr silicone catheter was cut into small pieces (25-30 mg) of length 3 cm. The ends of the catheters were blocked on both sides by heat-sealing them. The catheter surfaces were dip-coated and after air-drying, dried at 45 °C. 20 µL  $\sim 10^6$  CFU/mL *E. coli* R3336 bacteria was dropped on a petri dish. The surfaces were rigorously rubbed on the bacteria to smear the entire surface of the catheter. The uncoated catheter surface was the control for the experiment. The catheter surfaces were incubated at 37 °C for 45 minutes. Post-incubation the catheter surfaces were dragged across the diameter of the nutrient agar plate and kept for incubation for at 37 °C for 18 hrs. Photographic images were captured of the result. Also, another set of catheter surfaces were washed with 990 µL saline after incubation with the bacterial suspension. Serial dilution was conducted and 20 µL of the solutions were drop-casted on nutrient agar plates. The agar plates were incubated for 18 hours at 37 °C, consequently counting the bacterial colonies.

**2.5.2.8. Repeated Antibacterial Activity of Coated Surfaces.** The uncoated and coated catheters were washed with saline and water in 3 cycles for 1 minute each. After washing the surfaces, they were incubated with 20 µL  $\sim 10^6$  CFU/mL *E. coli* R3336 and *E. coli* MTCC 443 bacteria at 37 °C for 45 minutes. Once incubated, the surfaces were dragged across the agar plate and incubated at 37 °C for 18 hrs to check the antibacterial activity after washing the surfaces. Images were captured to investigate the result visually. A set of washed surfaces were used which were washed with 990 µL saline after incubation with the bacterial suspension.

Serial dilution was done, and the solutions were drop-casted on nutrient agar plates. The agar plates were incubated for 18 hrs at 37 °C, consequently counting the bacterial colonies.

#### **2.5.2.9. Bacterial Biofilm Inhibition Study.**

*Through Confocal imaging.* Glass coverslips of diameter 18mm were coated with **QPEI** by dissolving it in DCM and **APN<sub>3</sub>** solutions in DCM and DMSO (1:1) by drop-casting it on the surface. Thin films were obtained on the surface by air-drying them. Uncoated glass slips were used as the control in the experiment. The coverslips were placed into the wells of a 6-well plate. *E. coli* MTCC 443, *E. coli* R3336 and MRSA ATCC 33591 were suspended into suitable media (M9 media with 0.02% casamino acid 0.5% glycerol and nutrient broth supplemented with 1% NaCl and 1% glucose respectively). Bacterial solutions (2 mL) were then added to the wells containing the coverslips. The 6-well plates were incubated at 37 °C for 72 hrs under stationary conditions. Consequently, the coverslips were removed and washed with saline. The coverslips were finally placed on glass slides, green dye SYTO 9 (60 µM) solution, and red dye PI (15 µM) was added onto the coverslips and then air-sealed with another cover glass. The cover glasses were incubated for 15 minutes in the dark and imaged using a confocal laser scanning microscope (Zeiss LSM 800).

*Through counting of a bacterial colony.* **QPEI** was dissolved in DCM and **APN<sub>3</sub>** solutions in DCM and DMSO (1:1) were drop-cast on the surface of glass coverslips with a diameter of 18mm. By air-drying the surface, thin films were formed. The experiment employed uncoated glass slips as the control. In a 6-well plate, the coverslips were inserted into the wells. Suitable media were used to suspend *E. coli* MTCC 443, *E. coli* R3336 and MRSA ATCC 33591 bacteria (M9 media with 0.02 % casamino acid 0.5 % glycerol and nutrient broth supplemented with 1% NaCl and 1% glucose respectively). The coverslips were then placed in the wells with bacterial solutions (2 mL). Under stationary conditions, the 6-well plates were incubated at 37

°C for 72 hrs. After which, the coverslips were removed, and saline washed. Serial dilution was conducted with Trypsin EDTA and 20 µL of the resulting solutions were drop-casted on nutrient agar plates. The agar plates were incubated for 18 hrs at 37 °C, consequently counting the bacterial colonies.

**2.5.2.10. Antifungal Assay of Coated Surfaces by Dragging on YPD Plates.** 20 µL of  $\sim 10^6$  CFU/mL fungal suspension of *C. albicans* AB226 and *C. albicans* AB399 was dropped on 1x1 cm<sup>2</sup> coated and uncoated surfaces and covered with a coverslip and incubated at 37 °C for 2 hrs. The further process is similar to that described in the antibacterial assay of coated surfaces dragged on agar plates.

**2.5.2.11. Antifungal Assay.** Fungal strains *C. albicans* AB226 and *C. albicans* AB399 were streaked on yeast peptone dextrose (YPD) agar plates and incubated for 24 hrs at 30 °C. The single fungal colony was inoculated in 3 mL YPD media for 10 hrs at 37 °C to obtain the mid-log phase ( $\sim 10^8$  CFU/mL) of the fungal growth and eventually diluted to  $\sim 10^5$  CFU/mL in saline to experiment. The further process was similar to that of the antibacterial assay described previously.

**2.5.2.12. Fungicidal Kinetics.** 20 µL of  $\sim 10^6$  CFU/mL fungal suspension of *C. albicans* AB226 and *C. albicans* AB399 was dropped on 1x1 cm<sup>2</sup> coated and uncoated surfaces and covered with a coverslip and incubated at 37 °C for different time points 0, 30 minutes, 1 hr and 2 hrs. The pristine surfaces were used as the control for the experiment. The incubated surfaces were dragged across the YPD agar plates and incubated at 37 °C for 18 hrs. Photographs were captured for the visual results.

**2.5.2.13. Scanning Electron Microscopy Visualization of Bacterial Killing.** To observe the antibacterial activity of the coating, a previously established protocol was followed with certain modifications. 24-well plates were coated with APN<sub>3</sub>. Uncoated wells were treated as the

control for the experiment. A 400  $\mu\text{L}$  aliquot of  $\sim 10^7$  CFU/mL *E. coli* R3336 bacterial suspension in saline was added to the wells and incubated for 2 hrs at 37 °C. After the incubation period, the bacterial cells were transferred from the wells to a 1 mL centrifuge tube. Centrifugation was done at 3000 rpm for 5 minutes. The bacterial pellet obtained was resuspended in 30 % ethanol. Consequently, it was dehydrated with 50%, 70%, and 90% ethanol solution in water. Finally, the bacterial was resuspended in 90% ethanol. An aliquot of 5  $\mu\text{L}$  was drop-casted from the solution onto a silicon wafer and air-dried. The samples were gold-sputtered before imaging with Zeiss Gemini 500 FESEM.

**2.5.2.14. Live-Dead Assay of the Coating Against Bacteria.** A 96-well plate was taken, and 10 such wells were coated with **APN<sub>3</sub>**. 100  $\mu\text{L}$  of  $\sim 10^7$  CFU/mL bacterial solution of *E. coli* MTCC 443 was dropped into the 10 wells and kept for incubation at 37 °C for 60 minutes. After incubation period, the solutions were collected in an Eppendorf and allowed to centrifuge at 5000 rpm for 5 minutes. The supernatant was discarded, and the precipitate was dissolved in 1 mL of saline again. SYTO-9 (3  $\mu\text{M}$ ) and PI (15  $\mu\text{M}$ ) were added and kept for 15 minutes in the dark. The resultant solution was centrifuged again at 5000 rpm for 5 minutes. The supernatant was discarded and redissolved in 100  $\mu\text{L}$  saline. 5  $\mu\text{L}$  was drop-casted on a glass-slide for imaging. The same procedure was done for uncoated surfaces.

**2.5.2.15. ROS generation.** Surfaces coated with **QPEI**, ZnO and **APN<sub>3</sub>** solutions were incubated with 20  $\mu\text{L}$  of  $\sim 10^7$  CFU/mL bacterial solution of *E. coli* MTCC 443 at 37 °C for 10 minutes. Right after incubation, the surfaces were washed with 1 mL saline. Pristine surfaces were treated as control in the experiment. The washed solutions were treated with 10  $\mu\text{L}$  of 10  $\mu\text{M}$  2',7'-dichlorodihydrofluorescein diacetate (DCFDA) dye for staining. The sample were analysed for intracellular (reactive oxygen species) ROS generation through flow cytometry.



## References

- (1) Stamm, W. E.; Norrby, S. R. Urinary tract infections: disease panorama and challenges. *J. Infect. Dis.* **2001**, *183 Suppl 1*, S1–4.
- (2) Flores-Mireles, A. L.; Walker, J. N.; Caparon, M.; Hultgren, S. J. Urinary tract infections: epidemiology, mechanisms of infection and treatment options. *Nat. Rev. Microbiol.* **2015**, *13* (5), 269–284.
- (3) Klein, R. D.; Hultgren, S. J. Urinary tract infections: microbial pathogenesis, host-pathogen interactions and new treatment strategies. *Nat. Rev. Microbiol.* **2020**, *18* (4), 211–226.
- (4) Subashchandrabose, S.; Mobley, H. L. T. Virulence and Fitness Determinants of Uropathogenic Escherichia coli. *Microbiol. Spectr.* **2015**, *3* (4).
- (5) Song, J.; Bishop, B. L.; Li, G.; Grady, R.; Stapleton, A.; Abraham, S. N. TLR4-mediated expulsion of bacteria from infected bladder epithelial cells. *Proc. Natl. Acad. Sci. USA* **2009**, *106* (35), 14966–14971.
- (6) Anderson, G. G.; Palermo, J. J.; Schilling, J. D.; Roth, R.; Heuser, J.; Hultgren, S. J. Intracellular bacterial biofilm-like pods in urinary tract infections. *Science* **2003**, *301* (5629), 105–107.
- (7) Rosen, D. A.; Hooton, T. M.; Stamm, W. E.; Humphrey, P. A.; Hultgren, S. J. Detection of intracellular bacterial communities in human urinary tract infection. *PLoS Med.* **2007**, *4* (12), e329.
- (8) De Nisco, N. J.; Neugent, M.; Mull, J.; Chen, L.; Kuprasertkul, A.; de Souza Santos, M.; Palmer, K. L.; Zimmern, P.; Orth, K. Direct Detection of Tissue-Resident Bacteria and Chronic Inflammation in the Bladder Wall of Postmenopausal Women with Recurrent Urinary Tract Infection. *J. Mol. Biol.* **2019**, *431* (21), 4368–4379.
- (9) Robino, L.; Scavone, P.; Araujo, L.; Algorta, G.; Zunino, P.; Vignoli, R. Detection of intracellular bacterial communities in a child with Escherichia coli recurrent urinary tract infections. *Pathog Dis* **2013**, *68* (3), 78–81.
- (10) Robino, L.; Scavone, P.; Araujo, L.; Algorta, G.; Zunino, P.; Pérez, M. C.; Vignoli, R. Intracellular bacteria in the pathogenesis of Escherichia coli urinary tract infection in children. *Clin. Infect. Dis.* **2014**, *59* (11), e158–64.
- (11) Nicolle, L. E. Catheter associated urinary tract infections. *Antimicrob. Resist. Infect. Control* **2014**, *3*, 23.
- (12) Percival, S. L.; Suleman, L.; Vuotto, C.; Donelli, G. Healthcare-associated infections, medical devices and biofilms: risk, tolerance and control. *J. Med. Microbiol.* **2015**, *64* (Pt 4), 323–334.
- (13) Flores-Mireles, A. L.; Walker, J. N.; Bauman, T. M.; Potretzke, A. M.; Schreiber, H. L.; Park, A. M.; Pinkner, J. S.; Caparon, M. G.; Hultgren, S. J.; Desai, A. Fibrinogen

- Release and Deposition on Urinary Catheters Placed during Urological Procedures. *J. Urol.* **2016**, *196* (2), 416–421.
- (14) Kostakioti, M.; Hadjifrangiskou, M.; Hultgren, S. J. Bacterial biofilms: development, dispersal, and therapeutic strategies in the dawn of the postantibiotic era. *Cold Spring Harb. Perspect. Med.* **2013**, *3* (4), a010306.
- (15) Jacobsen, S. M.; Stickler, D. J.; Mobley, H. L. T.; Shirtliff, M. E. Complicated catheter-associated urinary tract infections due to *Escherichia coli* and *Proteus mirabilis*. *Clin. Microbiol. Rev.* **2008**, *21* (1), 26–59.
- (16) Trautner, B. W.; Darouiche, R. O. Role of biofilm in catheter-associated urinary tract infection. *Am. J. Infect. Control* **2004**, *32* (3), 177–183.
- (17) Magill, S. S.; Edwards, J. R.; Bamberg, W.; Beldavs, Z. G.; Dumyati, G.; Kainer, M. A.; Lynfield, R.; Maloney, M.; McAllister-Hollod, L.; Nadle, J.; et al. Multistate point-prevalence survey of health care-associated infections. *N. Engl. J. Med.* **2014**, *370* (13), 1198–1208.
- (18) Weiner, L. M.; Webb, A. K.; Limbago, B.; Dudeck, M. A.; Patel, J.; Kallen, A. J.; Edwards, J. R.; Sievert, D. M. Antimicrobial-Resistant Pathogens Associated With Healthcare-Associated Infections: Summary of Data Reported to the National Healthcare Safety Network at the Centers for Disease Control and Prevention, 2011-2014. *Infect. Control Hosp. Epidemiol.* **2016**, *37* (11), 1288–1301.
- (19) Guiton, P. S.; Hannan, T. J.; Ford, B.; Caparon, M. G.; Hultgren, S. J. *Enterococcus faecalis* overcomes foreign body-mediated inflammation to establish urinary tract infections. *Infect. Immun.* **2013**, *81* (1), 329–339.
- (20) Singha, P.; Locklin, J.; Handa, H. A review of the recent advances in antimicrobial coatings for urinary catheters. *Acta Biomater.* **2017**, *50*, 20–40.
- (21) Paladini, F.; Pollini, M.; Deponti, D.; Di Giancamillo, A.; Peretti, G.; Sannino, A. Effect of silver nanocoatings on catheters for haemodialysis in terms of cell viability, proliferation, morphology and antibacterial activity. *J Mater Sci Mater Med* **2013**, *24* (4), 1105–1112.
- (22) Ricardo, S. I. C.; Anjos, I. I. L.; Monge, N.; Faustino, C. M. C.; Ribeiro, I. A. C. A Glance at Antimicrobial Strategies to Prevent Catheter-Associated Medical Infections. *ACS Infect. Dis.* **2020**, *6* (12), 3109–3130.
- (23) Johnson, J. R.; Johnston, B.; Kuskowski, M. A. In vitro comparison of nitrofurazone- and silver alloy-coated foley catheters for contact-dependent and diffusible inhibition of urinary tract infection-associated microorganisms. *Antimicrob. Agents Chemother.* **2012**, *56* (9), 4969–4972.
- (24) Campoccia, D.; Montanaro, L.; Arciola, C. R. A review of the clinical implications of anti-infective biomaterials and infection-resistant surfaces. *Biomaterials* **2013**, *34* (33), 8018–8029.
- (25) Pai, M. P.; Pendland, S. L.; Danziger, L. H. Antimicrobial-coated/bonded and -impregnated intravascular catheters. *Ann. Pharmacother.* **2001**, *35* (10), 1255–1263.

- (26) Marconi, W.; Francolini, I.; Piozzi, A.; Rosa, R. D. Antibiotic releasing urethane polymers for prevention of catheter related infections. *J Bioact Compat Polym* **2001**, *16* (5), 393–407.
- (27) Desai, D. G.; Liao, K. S.; Cevallos, M. E.; Trautner, B. W. Silver or nitrofurazone impregnation of urinary catheters has a minimal effect on uropathogen adherence. *J. Urol.* **2010**, *184* (6), 2565–2571.
- (28) Regev-Shoshani, G.; Ko, M.; Crowe, A.; Av-Gay, Y. Comparative efficacy of commercially available and emerging antimicrobial urinary catheters against bacteriuria caused by *E. coli* in vitro. *Urology* **2011**, *78* (2), 334–339.
- (29) Kowalczyk, D.; Ginalska, G.; Piersiak, T.; Miazga-Karska, M. Prevention of biofilm formation on urinary catheters: comparison of the sparfloxacin-treated long-term antimicrobial catheters with silver-coated ones. *J. Biomed. Mater. Res. Part B Appl Biomater* **2012**, *100* (7), 1874–1882.
- (30) Dametto, F. R.; Ferraz, C. C. R.; Gomes, B. P. F. de A.; Zaia, A. A.; Teixeira, F. B.; de Souza-Filho, F. J. In vitro assessment of the immediate and prolonged antimicrobial action of chlorhexidine gel as an endodontic irrigant against *Enterococcus faecalis*. *Oral Surg. Oral Med. Oral Pathol. Oral Radiol. Endod.* **2005**, *99* (6), 768–772.
- (31) Slater-Radosti, C.; Van Aller, G.; Greenwood, R.; Nicholas, R.; Keller, P. M.; DeWolf, W. E.; Fan, F.; Payne, D. J.; Jaworski, D. D. Biochemical and genetic characterization of the action of triclosan on *Staphylococcus aureus*. *J. Antimicrob. Chemother.* **2001**, *48* (1), 1–6.
- (32) Petersen, R. C. Triclosan antimicrobial polymers. *AIMS Mol. Sci.* **2016**, *3* (1), 88–103.
- (33) Gaonkar, T. A.; Sampath, L. A.; Modak, S. M. Evaluation of the antimicrobial efficacy of urinary catheters impregnated with antiseptics in an in vitro urinary tract model. *Infect. Control Hosp. Epidemiol.* **2003**, *24* (7), 506–513.
- (34) Tian, Y.; Jian, Z.; Wang, J.; He, W.; Liu, Q.; Wang, K.; Li, H.; Tan, H. Antimicrobial activity Study of triclosan-loaded WBPU on *Proteus mirabilis* in vitro. *Int Urol Nephrol* **2017**, *49* (4), 563–571.
- (35) Kumar, R.; Münstedt, H. Silver ion release from antimicrobial polyamide/silver composites. *Biomaterials* **2005**, *26* (14), 2081–2088.
- (36) Knetsch, M. L. W.; Koole, L. H. New Strategies in the Development of Antimicrobial Coatings: The Example of Increasing Usage of Silver and Silver Nanoparticles. *Polymers (Basel)* **2011**, *3* (4), 340–366.
- (37) Pickard, R.; Lam, T.; MacLennan, G.; Starr, K.; Kilonzo, M.; McPherson, G.; Gillies, K.; McDonald, A.; Walton, K.; Buckley, B.; et al. Types of urethral catheter for reducing symptomatic urinary tract infections in hospitalised adults requiring short-term catheterisation: multicentre randomised controlled trial and economic evaluation of antimicrobial- and antiseptic-impregnated urethral catheters (the CATHETER trial). *Health Technol. Assess.* **2012**, *16* (47), 1–197.

- (38) Bhattacharjee, B.; Ghosh, S.; Patra, D.; Haldar, J. Advancements in release-active antimicrobial biomaterials: A journey from release to relief. *Wiley Interdiscip Rev Nanomed Nanobiotechnol* **2021**, e1745.
- (39) Ketchum, A. R.; Kappler, M. P.; Wu, J.; Xi, C.; Meyerhoff, M. E. The preparation and characterization of nitric oxide releasing silicone rubber materials impregnated with S-nitroso-tert-dodecyl mercaptan. *J. Mater. Chem. B, Mater. Biol. Med.* **2016**, *4* (3), 422–430.
- (40) Margel, D.; Mizrahi, M.; Regev-Shoshani, G.; Ko, M.; Moshe, M.; Ozalvo, R.; Shavit-Grievink, L.; Baniel, J.; Kedar, D.; Yossepowitch, O.; et al. Nitric oxide charged catheters as a potential strategy for prevention of hospital acquired infections. *PLoS One* **2017**, *12* (4), e0174443.
- (41) Ren, H.; Bull, J. L.; Meyerhoff, M. E. Transport of Nitric Oxide (NO) in Various Biomedical grade Polyurethanes: Measurements and Modeling Impact on NO Release Properties of Medical Devices. *ACS Biomater. Sci. Eng.* **2016**, *2* (9), 1483–1492.
- (42) Wo, Y.; Brisbois, E. J.; Wu, J.; Li, Z.; Major, T. C.; Mohammed, A.; Wang, X.; Colletta, A.; Bull, J. L.; Matzger, A. J.; et al. Reduction of Thrombosis and Bacterial Infection via Controlled Nitric Oxide (NO) Release from S-Nitroso-N-acetylpenicillamine (SNAP) Impregnated CarboSil Intravascular Catheters. *ACS Biomater. Sci. Eng.* **2017**, *3* (3), 349–359.
- (43) Cloutier, M.; Mantovani, D.; Rosei, F. Antibacterial coatings: challenges, perspectives, and opportunities. *Trends Biotechnol.* **2015**, *33* (11), 637–652.
- (44) Cheung, R. C. F.; Ng, T. B.; Wong, J. H.; Chan, W. Y. Chitosan: an update on potential biomedical and pharmaceutical applications. *Mar Drugs* **2015**, *13* (8), 5156–5186.
- (45) Kara, F.; Aksoy, E. A.; Yuksekdog, Z.; Aksoy, S.; Hasirci, N. Enhancement of antibacterial properties of polyurethanes by chitosan and heparin immobilization. *Appl Surf Sci* **2015**, *357*, 1692–1702.
- (46) Campana, R.; Casettari, L.; Ciandrini, E.; Illum, L.; Baffone, W. Chitosans inhibit the growth and the adhesion of *Klebsiella pneumoniae* and *Escherichia coli* clinical isolates on urinary catheters. *Int. J. Antimicrob. Agents* **2017**, *50* (2), 135–141.
- (47) Jiao, Y.; Niu, L.-N.; Ma, S.; Li, J.; Tay, F. R.; Chen, J.-H. Quaternary ammonium-based biomedical materials: State-of-the-art, toxicological aspects and antimicrobial resistance. *Prog Polym Sci* **2017**, *71*, 53–90.
- (48) Kaur, R.; Liu, S. Antibacterial surface design – Contact kill. *Prog Surf Sci* **2016**, *91* (3), 136–153.
- (49) Babutan, I.; Lucaci, A.-D.; Botiz, I. Antimicrobial polymeric structures assembled on surfaces. *Polymers (Basel)* **2021**, *13* (10).
- (50) Cyphert, E. L.; von Recum, H. A. Emerging technologies for long-term antimicrobial device coatings: advantages and limitations. *Exp. Biol. Med.* **2017**, *242* (8), 788–798.

- (51) Pant, J.; Gao, J.; Goudie, M. J.; Hopkins, S. P.; Locklin, J.; Handa, H. A multi-defense strategy: Enhancing bactericidal activity of a medical grade polymer with a nitric oxide donor and surface-immobilized quaternary ammonium compound. *Acta Biomater.* **2017**, *58*, 421–431.
- (52) Lakshmaiah Narayana, J.; Chen, J.-Y. Antimicrobial peptides: Possible anti-infective agents. *Peptides* **2015**, *72*, 88–94.
- (53) Yu, K.; Lo, J. C. Y.; Yan, M.; Yang, X.; Brooks, D. E.; Hancock, R. E. W.; Lange, D.; Kizhakkedathu, J. N. Anti-adhesive antimicrobial peptide coating prevents catheter associated infection in a mouse urinary infection model. *Biomaterials* **2017**, *116*, 69–81.
- (54) Mishra, B.; Lushnikova, T.; Golla, R. M.; Wang, X.; Wang, G. Design and surface immobilization of short anti-biofilm peptides. *Acta Biomater.* **2016**, *49*, 316–328.
- (55) Bazaka, K.; Jacob, M. V.; Chrzanowski, W.; Ostrikov, K. Anti-bacterial surfaces: natural agents, mechanisms of action, and plasma surface modification. *RSC Adv.* **2015**, *5* (60), 48739–48759.
- (56) Simões, N. G.; Bettencourt, A. F.; Monge, N.; Ribeiro, I. A. C. Novel antibacterial agents: an emergent need to win the battle against infections. *Mini Rev. Med. Chem.* **2017**, *17* (14), 1364–1376.
- (57) Monteiro, C.; Costa, F.; Pirttilä, A. M.; Tejesvi, M. V.; Martins, M. C. L. Prevention of urinary catheter-associated infections by coating antimicrobial peptides from crowberry endophytes. *Sci. Rep.* **2019**, *9* (1), 10753.
- (58) Wang, Y.; Kotsuchibashi, Y.; Liu, Y.; Narain, R. Study of bacterial adhesion on biomimetic temperature responsive glycopolymer surfaces. *ACS Appl. Mater. Interfaces* **2015**, *7* (3), 1652–1661.
- (59) Grumezescu, V.; Holban, A. M.; Sima, L. E.; Chiritoiu, M. B.; Chiritoiu, G. N.; Grumezescu, A. M.; Ivan, L.; Safciuc, F.; Antohe, F.; Florica, C.; et al. Laser deposition of poly(3-hydroxybutyric acid-co-3-hydroxyvaleric acid) - lysozyme microspheres based coatings with anti-microbial properties. *Int. J. Pharm.* **2017**, *521* (1-2), 184–195.
- (60) Ivanova, K.; Fernandes, M. M.; Mendoza, E.; Tzanov, T. Enzyme multilayer coatings inhibit *Pseudomonas aeruginosa* biofilm formation on urinary catheters. *Appl. Microbiol. Biotechnol.* **2015**, *99* (10), 4373–4385.
- (61) Hoque, J.; Yadav, V.; Prakash, R. G.; Sanyal, K.; Haldar, J. Dual-Function Polymer-Silver Nanocomposites for Rapid Killing of Microbes and Inhibiting Biofilms. *ACS Biomater. Sci. Eng.* **2019**, *5* (1), 81–91.
- (62) Hoque, J.; Akkapeddi, P.; Ghosh, C.; Uppu, D. S. S. M.; Haldar, J. A Biodegradable Polycationic Paint that Kills Bacteria in Vitro and in Vivo. *ACS Appl. Mater. Interfaces* **2016**, *8* (43), 29298–29309.

- (63) Darbasizadeh, B.; Fatahi, Y.; Feyzi-Barnaji, B.; Arabi, M.; Motasadizadeh, H.; Farhadnejad, H.; Moraffah, F.; Rabiee, N. Crosslinked-polyvinyl alcohol-carboxymethyl cellulose/ZnO nanocomposite fibrous mats containing erythromycin (PVA-CMC/ZnO-EM): Fabrication, characterization and in-vitro release and anti-bacterial properties. *Int. J. Biol. Macromol.* **2019**, *141*, 1137–1146.
- (64) Kurowska, M.; Eickenscheidt, A.; Al-Ahmad, A.; Lienkamp, K. Simultaneously Antimicrobial, Protein-Repellent, and Cell-Compatible Polyzwitterion Networks: More Insight on Bioactivity and Physical Properties. *ACS Appl. Bio Mater.* **2018**, *1* (3), 613–626.
- (65) Jiang, L.; Loo, S. C. J. Intelligent Nanoparticle-Based Dressings for Bacterial Wound Infections. *ACS Appl. Bio Mater.* **2021**, *4* (5), 3849–3862.
- (66) Nishimoto, S.; Bhushan, B. Bioinspired self-cleaning surfaces with superhydrophobicity, superoleophobicity, and superhydrophilicity. *RSC Adv.* **2013**, *3* (3), 671–690.
- (67) Reddy, S. T.; Chung, K. K.; McDaniel, C. J.; Darouiche, R. O.; Landman, J.; Brennan, A. B. Micropatterned surfaces for reducing the risk of catheter-associated urinary tract infection: an in vitro study on the effect of sharklet micropatterned surfaces to inhibit bacterial colonization and migration of uropathogenic *Escherichia coli*. *J Endourol* **2011**, *25* (9), 1547–1552.
- (68) Hoque, J.; Ghosh, S.; Paramanandham, K.; Haldar, J. Charge-Switchable Polymeric Coating Kills Bacteria and Prevents Biofilm Formation in Vivo. *ACS Appl. Mater. Interfaces* **2019**, *11* (42), 39150–39162.
- (69) Schwartz, V. B.; Thétiot, F.; Ritz, S.; Pütz, S.; Choritz, L.; Lappas, A.; Förch, R.; Landfester, K.; Jonas, U. Antibacterial Surface Coatings from Zinc Oxide Nanoparticles Embedded in Poly(N-isopropylacrylamide) Hydrogel Surface Layers. *Adv. Funct. Mater.* **2012**, *22* (11), 2376–2386.
- (70) Sirelkhatim, A.; Mahmud, S.; Seeni, A.; Kaus, N. H. M.; Ann, L. C.; Bakhori, S. K. M.; Hasan, H.; Mohamad, D. Review on Zinc Oxide Nanoparticles: Antibacterial Activity and Toxicity Mechanism. *Nano-Micro Lett.* **2015**, *7* (3), 219–242.
- (71) Fisher, R. A.; Gollan, B.; Helaine, S. Persistent bacterial infections and persister cells. *Nat. Rev. Microbiol.* **2017**, *15* (8), 453–464.
- (72) Gaston, J. R.; Johnson, A. O.; Bair, K. L.; White, A. N.; Armbruster, C. E. Polymicrobial interactions in the urinary tract: is the enemy of my enemy my friend? *Infect. Immun.* **2021**.
- (73) Mukherjee, S.; Ghosh, S.; Haldar, J. Amphiphilic cationic macromolecule potentiates tetracycline against multi-drug resistant Gram-negative bacteria. *Bull. Mater. Sci.* **2020**, *43* (1), 311.
- (74) Birben, E.; Sahiner, U. M.; Sackesen, C.; Erzurum, S.; Kalayci, O. Oxidative stress and antioxidant defense. *World Allergy Organiz J* **2012**, *5* (1), 9–19.

- (75) Eruslanov, E.; Kusmartsev, S. Identification of ROS using oxidized DCFDA and flow-cytometry. *Methods Mol. Biol.* **2010**, *594*, 57–72.





## **Publications**

- Bhattacharjee, B.; Ghosh, S.; **Patra, D.**; Haldar, J. Advancements in release-active antimicrobial biomaterials: A journey from release to relief. *Wiley Interdiscip Rev Nanomed Nanobiotechnol* **2021**, e1745.
- Ghosh, S.; Mukherjee, S.; **Patra, D.**; Haldar, J. Polymeric Biomaterials for Prevention and Therapeutic Intervention of Microbial Infections. *Biomacromolecules* **2022**, *23*, 592-608.
- **Patra, D.**; Haldar, J. Antimicrobial Polymer-Zinc Oxide Nanocomposite Coatings for Rapid Intervention of CAUTIs. *Manuscript under preparation*.